NASA CR-167873

(NASA-CR-167873) ATMOSPHERIC RADIATION MODEL FOR WATER SURFACES Final Technical Report, 4 Mar. 1981 - 15 Jul. 1982 (Science Applications, Inc.) 67 p HC A04/MF A01 CSCL 04A G3/46

N83-21677

Unclas 03211

SCIENCE APPLICATIONS, INC.

NASA CR-167873
SAI-82-002-AA

ATMOSPHERIC RADIATION MODEL FOR WATER SURFACES

FINAL TECHNICAL REPORT

ROBERT E. TURNER
DANIEL W. GASKILL
JAMES R. LIERZER

SCIENCE APPLICATIONS, INC.
1010 WOODMAN DRIVE, SUITE 200
DAYTON, OHIO 45432

MAY 1982

PREPARED FOR
NATIONAL AERONAUTICS AND SPACE ADMINISTRATION
LEWIS RESEARCH CENTER
CLEVELAND, OHIO 44135
CONTRACT NO. NAS3-22495

UNCLASSIFIED

SECURITY CLASSIFICATION OF THIS PAGE (When Data Entered)

REPORT DOCUMENTATION PAGE		READ INSTRUCTIONS BEFORE COMPLETING FORM
1. REPORT NUMBER NASA CR-167873	2. GOVT ACCESSION NO.	3. RECIPIENT'S CATALOG NUMBER
4. TITLE (and Subtitle) "ATMOSPHERIC RADIATION MODEL FOR WATER SURFACES"		5. TYPE OF REPORT & PERIOD COVERED Final Technical Report 4 March 81 - 15 July 82
		6. PERFORMING ORG. REPORT NUMBER SAI-82-002-AA
7. AUTHOR(s) Robert E. Turner Daniel W. Gaskill James R. Lierzer		8. CONTRACT OR GRANT NUMBER(s) NAS3-22495
9. PERFORMING ORGANIZATION NAME AND ADDRESS Science Applications, Incorporated 15 Research Drive Ann Arbor, Michigan 48103		10. PROGRAM ELEMENT, PROJECT, TASK AREA & WORK UNIT NUMBERS
11. CONTROLLING OFFICE NAME AND ADDRESS NASA - Lewis Research Center 21000 Brookpark Road Cleveland, Ohio 44135		12. REPORT DATE May 1982
		13. NUMBER OF PAGES ix + 56
14. MONITORING AGENCY NAME & ADDRESS (if different from Controlling Office)		15. SECURITY CLASS. (of this report) Unclassified
		15a. DECLASSIFICATION/DOWNGRADING SCHEDULE

16. DISTRIBUTION STATEMENT (of this Report)

ORIGINAL PAGE IS
OF POOR QUALITY

17. DISTRIBUTION STATEMENT (of the abstract entered in Block 20, if different from Report)

18. SUPPLEMENTARY NOTES

Mr. Thom Coney was the Technical Monitor.

19. KEY WORDS (Continue on reverse side if necessary and identify by block number)

Aerosol	Radiative Transfer
Algorithm	Reflectance
Atmospheric Scattering	Radiance
Particulates	Water Surface

20. ABSTRACT (Continue on reverse side if necessary and identify by block number)

The purpose of this investigation is to extend an atmospheric correction model to account for various atmospheric radiation components in remotely sensed data. A previous study considered the path radiance which results from singly and multiply scattered radiation along the line of sight from a multispectral aircraft sensor and a target on a water surface. This report considers

DD FORM 1 JAN 73 1473 EDITION OF 1 NOV 65 IS OBSOLETE UNCLASSIFIED additional components such as the atmospheric path radiance which results from singly-scattered sky radiation specularly reflected by the water surface. It also considers a component which is referred to as the virtual sun path radiance, i.e. the singly-scattered path radiance which results from the solar radiation which is specularly reflected by the water surface.

These atmospheric radiation components are coded into a computer program for the analysis of multispectral remote sensor data over the Great Lakes of the United States. The user must know certain parameters, such as the visibility or spectral optical thickness of the atmosphere and the geometry of the sensor with respect to the sun and the target elements under investigation.

Suggestions and recommendations are given for further investigation of the problem of the remote sensing of water surfaces. If all of these extrinsic radiation components are properly accounted for, then the intrinsic water radiance can be found by applying the algorithm or an adaptation of the algorithm in this report. As a result, one would then be able to know the actual surface water spectral radiation field independent of the atmosphere.

PREFACE

This report describes part of the work done on a research program in the remote sensing of the Great Lakes using a multispectral scanner aboard an aircraft. The research has been conducted for the NASA-Lewis Research Center, Cleveland, Ohio, by Science Applications, Inc., at the Dayton, Ohio, office. The primary objective of this program is to develop remote sensing as a practical technique for the analysis of the Great Lakes.

Remote sensing of the environment involves the transfer of radiation from the Earth's surface through the atmosphere to a sensor which is located at some point within the atmosphere. For water surfaces with their inherently low reflectances, the atmospheric scattering of solar radiation acts as a significant noise factor. In this report we have extended an existing model to include various atmospheric radiation components so that the resulting mathematical algorithm will allow one to extract a radiance value which is more nearly representative of the actual radiance of the water, independent of atmospheric effects.

This research was performed under contract NAS3-22495 and covers the period from 4 March 1981 through 15 July 1982. Mr. Thom Coney served as Technical Monitor of the contract and Dr. Robert E. Turner of Science Applications, Inc., was the program manager and principal investigator.

CONTENTS

FIGURES

FIGURES (Cont'd)

TABLES

SYMBOLS

E_0	solar irradiance at the top of the atmosphere
E_0'	solar irradiance of the virtual sun
$L_0(i)$	radiance incident at angle i
$L_s(i)$	surface radiance at angle i
L_{SKYRE}	reflected sky radiance
L_{SOLRE}	reflected solar radiance
L_{SKY}	sky radiance
L_{SOL}	direct beam radiance
L_{PMS}	multiply scattered path radiance
L_{PSS}	singly scattered path radiance
L_U	upward scattered radiance beneath water surface
L_{INIR}	radiance scattered from beneath water surface
L_{SKYSS}	singly scattered sky radiance
L_{PTOT}	total radiance
L_{VSOL}	radiance from virtual sun
L_{VP}	virtual sun path radiance
n	index of refraction of water relative to air
p	slope probability
$p(\chi)$	scattering phase function
T	transmittance

(GREEK SYMBOLS)

θ_i	incident angle
θ_r	reflected angle
ρ_s	Fresnel reflectance

$\rho_f(i)$	Fresnel reflectance at angle i
θ	nadir view angle
θ_0	solar zenith angle
ϕ	azimuth view angle
ϕ_0	solar azimuth angle
μ	cosine of nadir view angle
μ_o	cosine of solar zenith angle
χ_{SKY}	scattering angle
τ	optical depth
τ_0	optical thickness
η	forward scattering parameter
ρ	surface albedo
ω_0	single scattering albedo

SUMMARY

In the analysis of remotely sensed data on bodies of water, the atmosphere obscures the inherent surface features as a result of the scattering and absorption of solar radiation. In the case of multispectral data acquired by aircraft or spacecraft sensors, one can preprocess the data by applying mathematical models and algorithms to the digitized data. The mathematical model developed in this investigation is specifically designed to account for various components of the visible and infrared radiation in the atmosphere which interfere with the inherent signal from a water surface. If the atmospheric parameters are known, then when the algorithm is applied to the multispectral data sets, an improved or corrected data set will result.

This improved atmospheric correction model allows for the path radiance in the atmosphere as a result of singly-scattered solar radiation and also singly-scattered solar-reflected radiation. In addition, the model includes a singly-scattered sky radiation component for the radiation which is reflected by the water surface. Comparisons are made among the relative magnitudes of these radiation components in terms of the geometric and environmental factors. Recommendations are presented for a more advanced model which would include the corresponding radiation components for multiple scattering.

INTRODUCTION

Multispectral scanner data obtained by sensors aboard aircraft and spacecraft allow a user to examine the detailed physical properties of a surface. These properties are of interest to many investigations in various disciplines such as land use studies, agriculture, hydrology, forestry, and oceanography. In all of these investigations, however, the scattering of visible and infrared radiation by the atmospheric constituents will reduce the inherent surface radiance and add a path radiance to the attenuated radiance from the target. For many cases of the remote sensing of bright land areas on relatively clear days the attenuated radiation from the surface is rather large as compared to the atmospheric path radiance. For water bodies, with inherently low reflectances, this is no longer true and the path radiance can be a major effect in the total radiance at the sensor.

The purpose of this investigation was to extend an existing atmospheric radiative transfer model to include other radiation components which did not exist in the previous model. These additional atmospheric radiation components include specific effects for the remote sensing of water surfaces. The model is used in conjunction with an algorithm specifically designed for the analysis of multispectral data.

The determination of the atmospheric radiation components is important for the analysis of the probability of misclassification of various classes of surface materials. To first order one may consider the so called linear transfer problem in which the path radiance is constant over varying surface reflectances for a horizontally spatially uniform haze. For a non-uniform haze, however, the path radiance can vary, thereby resulting in a higher probability of misclassification of objects if the degree of non-uniformity is unknown. A second-order effect, but one which can become quite important for the remote sensing of high-contrast targets is the adjacency effect. This is when radiation from a bright target causes an increase in the path radiance with respect to the radiance from a neighboring dark target. This problem would exist, for example, in the remote sensing of water bodies near bright sandy beaches. The results should be evident in the brightened image of the water near the shoreline, provided the effects of waves and whitecaps are eliminated. This second-order adjacency effect is not included in the model or algorithm in this investigation but the effect can be accounted for if the investigator has sufficiently detailed atmospheric data on the horizontal stratification of aerosols.

Multiple scattering is particularly important if the sky is hazy. These effects are considered in the model for path radiance which results from the sun as a source. We have not included the multiple scattering effects for solar-reflected radiation.

3
OPTICAL PROPERTIES OF WATER

The interpretation of remote sensing data collected over water surfaces requires a detailed knowledge of the optical properties of water and the air-water interface. Water is unusual as a natural surface because it is a specular reflector and because in the visible regions sensible data can be obtained from well below the water surface [1]. Also of importance is the phenomenon of refraction, which occurs when radiation passes through the air-water boundary. These properties of water and their significance in terms of remote sensing are discussed in detail in this chapter.

3.1 REFLECTION, REFLECTANCE AND REFRACTION

Most natural surfaces are approximately Lambertian--reflecting incident radiance equally in all directions. A smooth water surface, however, is a specular reflector, and reflection of radiation from it follows the geometrical law of reflection. This geometric law requires that the angle with respect to the normal to the surface of the reflected ray equal the angle of incidence of the incident ray and that the reflected ray be in the same plane as the incident ray. Specular reflection is depicted in Figure 1. Reflectance, ρ_s, of the water surface is given by the Fresnel equation

$$\rho_s = \frac{1}{2}\left[\frac{\sin^2(\theta_i-\theta_r)}{\sin^2(\theta_i+\theta_r)} + \frac{\tan^2(\theta_i-\theta_r)}{\tan^2(\theta_i+\theta_r)}\right], \quad (1)$$

where θ_i is the incident angle and θ_r is the angle of refraction.

The transmitted part of the incident ray experiences refraction at the water surface, as shown in Figure 2. Snell's law, given by

$$\frac{\sin(\theta_i)}{\sin(\theta_r)} = n, \quad (2)$$

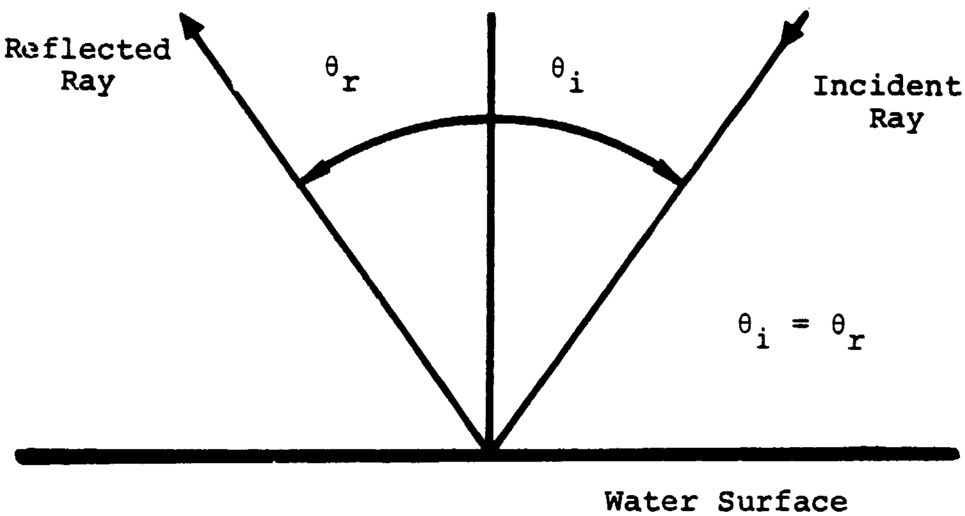

FIGURE 1. SPECULAR REFLECTION FROM A SMOOTH WATER SURFACE. THE INCIDENT AND REFLECTED RAYS ARE IN THE SAME PLANE.

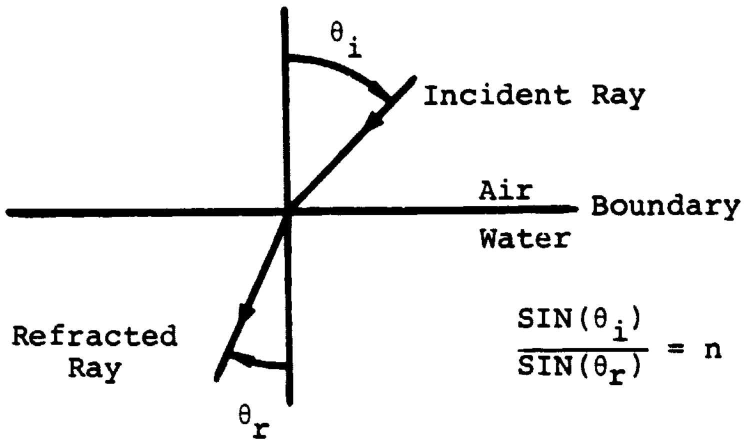

$$\frac{\mathrm{SIN}(\theta_i)}{\mathrm{SIN}(\theta_r)} = n \text{ (Snell's law)}$$

FIGURE 2. REFRACTION OF THE TRANSMITTED BEAM AT THE WATER SURFACE AND THE LAW OF REFRACTION
n = REFRACTIVE INDEX OF WATER RELATIVE TO AIR.

describes the relationship between the angle of incidence of the incoming beam, θ_i, the angle with respect to the normal to the surface of the refracted beam, θ_r, and the refractive index of air relative to water. The refracted beam lies in the same plane as the incident beam. The phenomenon of refraction is depicted in Figure 2. The law of refraction requires that for a water surface, downward sky radiation and direct sunlight enter the water within 48.5° of the vertical. Only when the water surface is roughened by wind or another disturbance can direct sunlight or sky radiation penetrate the water surface outside this range of angles. Back-scattered radiation from beneath the water-air interface also experiences refraction on reaching the water surface. When the water surface is calm, upward radiation incident at angles greater than 48.5° with the vertical is totally internally reflected [2]. Thus, downward radiation beneath the water surface at angles with the vertical greater than 48.5° is upward radiation in the water which has been totally internally reflected [3].

Equations 1 and 2 show that the reflectance and transmittance of the water surface are dependent on the refractive index of water. The refractive index is influenced by changes in temperature and by the concentration of various solutes in the water. Figure 3 shows how the reflectance function, equation 1, varies as a function of the angle of incidence for refractive indices of 1.20, 1.33, 1.40, 1.45. This range of refractive indices encompasses the range of natural variability in the refractive index for water; and Figure 3 shows that, over this range, variation in the refractive index is of little importance in determining the surface reflectance. For all of the calculations shown in this report, a refractive index of 4/3 is used. Figure 4 shows transmittance, T, and reflectance, ρ_s, as a function of angle of incidence of the incoming radiation for a refractive index of 1.33.

Since many applications of remote sensing over water require

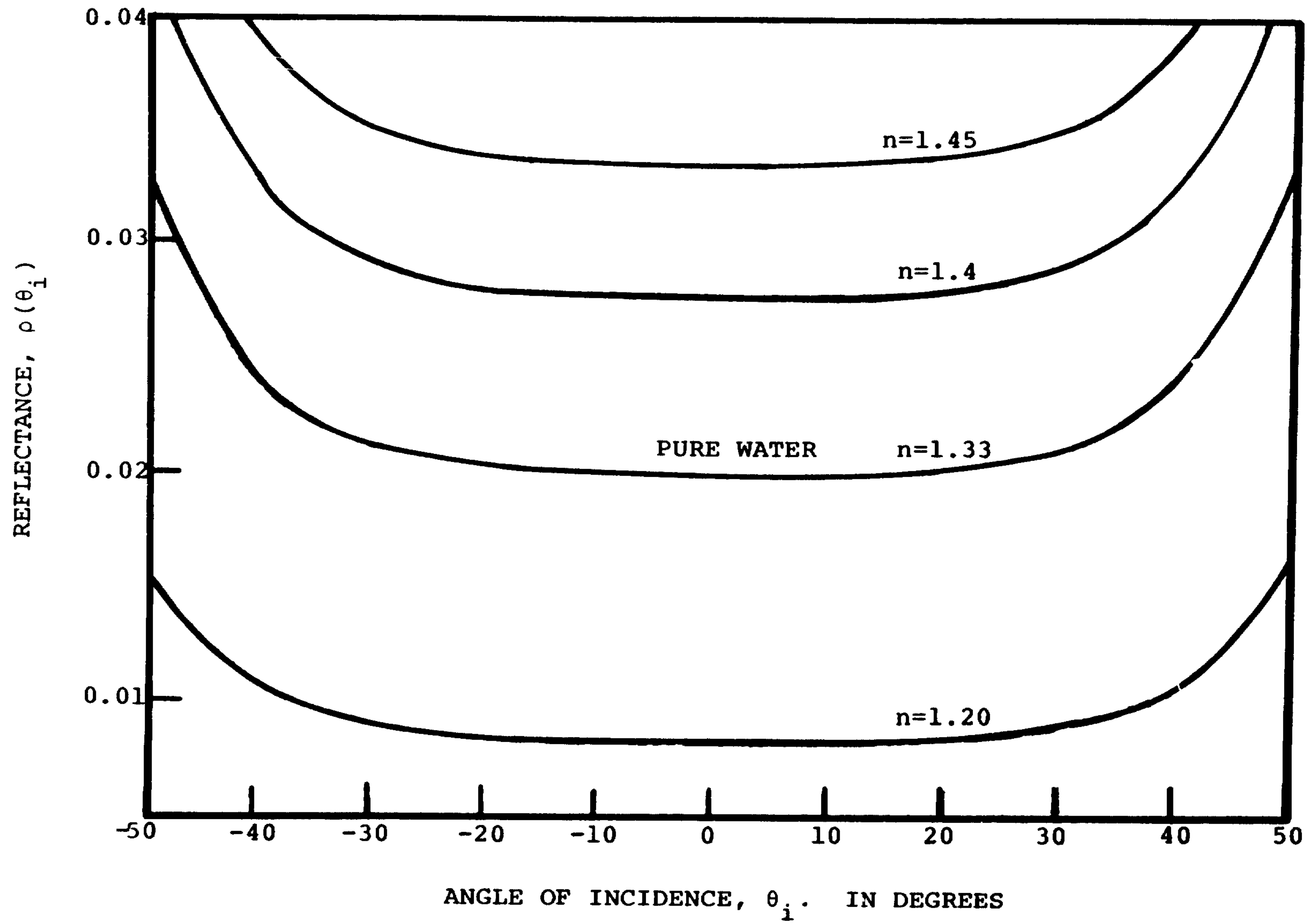

n = INDEX OF REFRACTION

FIGURE 3. FRESNEL REFLECTANCE FOR UNPOLARIZED LIGHT AS A FUNCTION OF ANGLE OF INCIDENCE OF INCOMING BEAM.

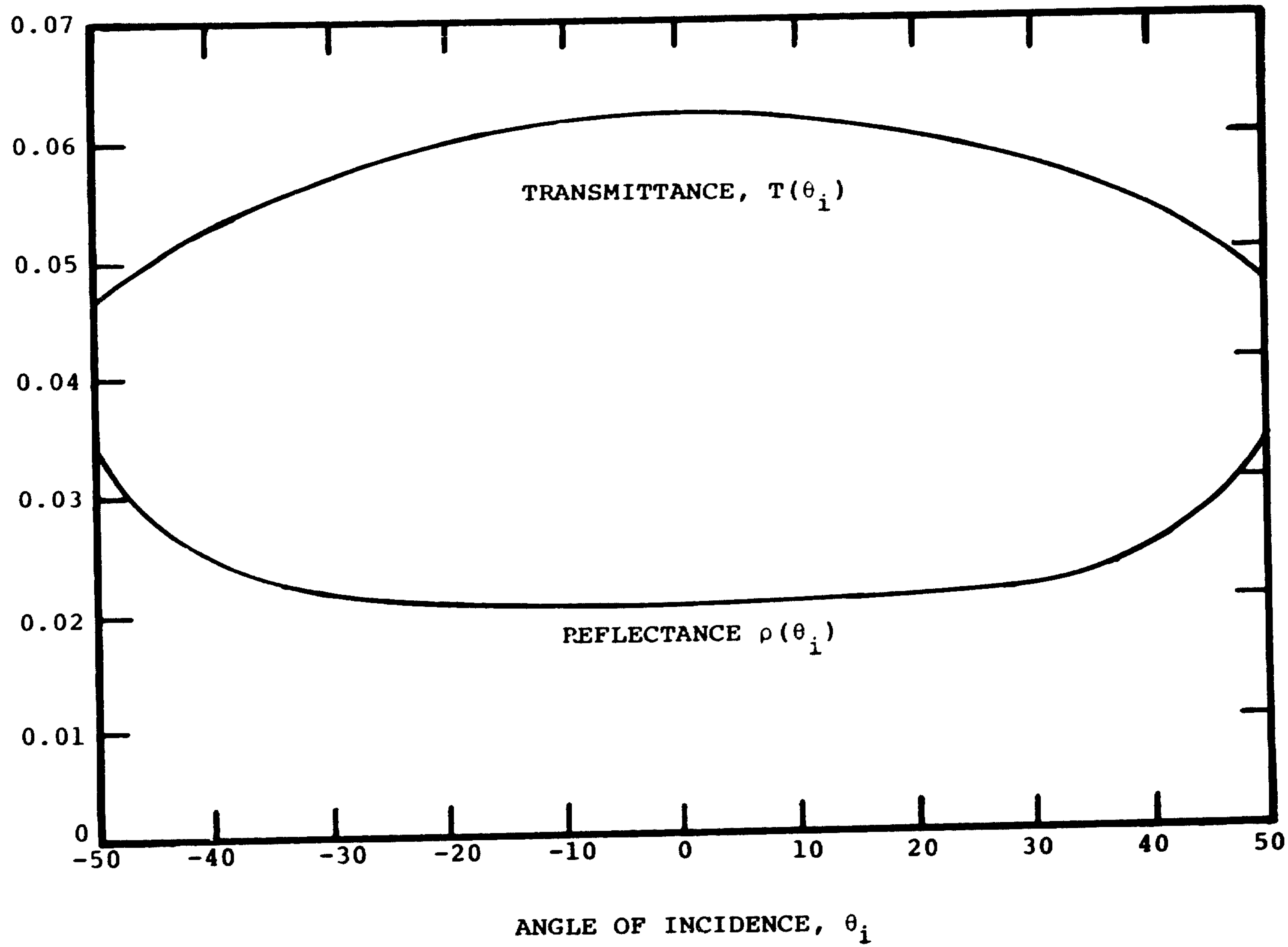

FIGURE 4. FRESNEL REFLECTANCE AND TRANSMITTANCE AS A FUNCTION OF ANGLE OF INCIDENCE OF INCOMING BEAM. REFRACTIVE INDEX = 1.33.

examining the signature from beneath the water surface, Fresnel reflectance is of paramount importance. Figure 4 shows that transmittance is highest when the incident beam is perpendicular to the water surface, while the reflectance is lowest at this angle. Thus, from a consideration of the Fresnel formulas, one would expect the return from beneath the water surface relative to the total, to be greatest when viewing that surface at the nadir. Contributing to this effort is the fact that most scattering phase functions for polydispersions in water have a secondary peak at 180^0 [2]. Figure 4 shows that while the Fresnel reflectance function is at a minimum at the nadir view angle, this function changes very little out to viewing angles as great as 40^0, at which point it begins to rise steeply. Internal reflection at the water surface of upwelling radiation is also at a minimum normal to the water surface. Thus, for remote sensing work where the return from beneath the water surface is of greatest interest, scan angles should be maintained within 40^0 to 45^0 of the vertical. Beyond an angle of 48.5^0 no radiation from beneath the water surface will reach the sensor when the water surface is calm. Scanning in the solar plane is also problematic in this regard since specularly reflected light on the solar side of the scan plane would saturate the sensor. For some purposes, such as viewing the glitter pattern on the water surface, scanning in the solar plane may be desirable.

3.2 ABSORPTION AND SCATTERING

Water is a good absorber of electromagnetic radiation. Only in the relatively narrow spectral region from about 400 to 600 nanometers is the transparency of water such that radiation can penetrate more than a few meters in depth below the water surface. Both at wavelengths shorter than 400 nm and longer than 600 nm, absorption increases rapidly and only very small amounts of radiation are scattered back out of the water into the atmosphere. At the very short wavelengths this radiation is further strongly attenuated in the atmosphere.

Scattering of radiation in water is caused by water molecules, by dissolved salts and by particles in suspension. These effects are usually assumed to be additive [4].

Scattering by water molecules is described by fluctuation theory which predicts scattering of radiation as a result of molecular movements which cause fluctuations in the density of the medium. As in Rayleigh scattering, this type of scattering is proportional to λ^{-4}, where λ is the wavelength of the radiation being scattered. The effect of dissolved salts on the molecular scattering phase function is usually small enough to be neglected.

In general, most scattering in water is accomplished by particles in suspension [4]. Particulate matter in water derives from runoff from land, deposition from the atmosphere, and organic processes within the water. Thus, particles may be quite irregular in shape and particle size distributions are difficult to characterize precisely [2]. Because some sources of particles such as runoff of organic processes may be highly localized in space, size distributions may vary greatly in space and time. Although particle shapes vary considerably from the spherical ideal of scattering theory, it has been shown [5,6] that systems of irregularly shaped particles can be adequately approximated by systems of polydisperse systems of spherical particles. The major observed features of phase functions of particulate suspensions in water are a strong forward scattering peak, a broad minimum around 100°-130° and a small secondary peak in the back scattering direction [4].

3.3 OPTICAL PROPERTIES OF A WIND ROUGHENDED WATER SURFACE

Roughness of the water surface caused by wind presents an additional problem in the calculation of the optical properties of the surface. Waves increase the angle of incidence of direct radiation for high solar elevations. The effect on the Fresnel reflectance, however, is of little consequence since the reflectance does not vary much with solar zenith angle for zenith angles less than 40^0 (see Figure 3). Waves reduce the angle of incidence of direct radiation from a low sun, greatly reducing the reflectance of the water surface. Cox and Munk [7] have shown that wave action becomes a significant factor for solar elevations below 20^0. At these low sun elevations, reduced reflection, shadowing and multiple reflections greatly reduce the reflected radiance.

The reflection of diffuse radiation by the water surface is little affected by surface roughness [2] , although complete agreement on this matter is lacking [8]. Burt [9] found that the albedo of a wind roughened water surface was slightly less than the albedo of a smooth water surface--a decrease from 6.6% to 5.7% for the roughened surface. Cox and Munk [7] measured a small increase in the albedo of a smooth water surface of 5% to 5.5% for a water surface roughened by waves. Kondratyev [8] on the other hand, calculates that where the solar zenith angle is 0^0 the albedo of calm water surface of 2.1% will increase to 13.1%. When the solar zenith angle is 30^0, the increase will be from 2.2% to 3.8%, and for a solar zenith angle of 60^0 there will be a decrease from 6.2% down to 2.4% for a roughened surface. Plass et al. [10], using a Monte Carlo model of the atmosphere ocean system, demonstrate that the downward flux just below the surface always increases with wind speed, even at high sun elevations. They attribute this result to the fact that more sky radiance near the horizon enters the water when waves are present.

The effect of waves on the radiance of the water surface can be calculated if the probability distribution of surface slopes is known. For an observer looking down on a water surface, the specular angle will vary from place to place over the surface of the water. Since in most remote sensing applications the light source (Sun) and observer (sensor) are high enough above the surface and the region viewed sufficiently small that variation in the specular angle can be neglected. The radiance of the surface is then directly proportional to the probability of finding a surface element with slope, S_0, at the specular angle [11]. If p is this probability, the radiance of the surface, L_s, at vertical angle i is given by

$$L_s(i) = L_0(i)\rho_f(i)p \quad (3)$$

where

$L_0(i)$ is radiance incident at the surface at vertical angle i, and

$\rho_f(i)$ is the Fresnel reflectance at vertical angle i.

Duntley [12] and Cox and Munk [7,13] have studied the statistical distribution of wave slope as a function of wind speed. Observations of the effect of wind speed on spatially or temporally averaged reflectance of the water surface indicate that it is not significant for view angles less than 70^0 from vertical. Angles in excess of 50^0 from the vertical are seldom used in remote sensing systems because of the large optical air mass at these angles.

4
COMPONENTS OF REFLECTED AND PATH RADIANCE IN REMOTE SENSING OVER WATER

In many applications of oceanographic remote sensing the quantity of greatest interest is the radiance information transmitted from below the water surface to a sensor, sometimes called the intrinsic radiance. To determine this quantity from raw remote sensing data we must not only estimate atmospheric path radiance but also the magnitude of radiance reflected off the water surface and transmitted to the sensor. In this chapter we describe in detail analytical models appropriate for estimating the following quantities: reflected sky radiance, L_{SKYRE}; singly scattered reflected solar path radiance, L_{VP}; singly scattered path radiance, L_{PSS}; and multiply scattered path radiance, L_{PMS}. The first two of these quantities are radiances resulting from specular reflection off the water surface, the latter two are atmospheric path radiances. Each of these radiances augments the radiance detected by a sensor, masking the radiance signal from beneath the water surface, as shown in Figure 5.

4.1 REFLECTED SKY RADIANCE, L_{SKYRE}

The geometry for sky radiance reflected into the line of sight of the sensor is depicted in Figure 6, where θ represents the nadir view angle of the sensor, ϕ the azimuth of the sensor scanning plane. We assume a plane parallel uniform atmosphere. Sky radiance downwelling in the scan plane and incident at an angle θ with the normal to the surface is reflected in the direction of the sensor, and attenuated by the atmosphere as it travels to the sensor. The surface reflectance is given by the Fresnel formula for unpolarized light described in Chapter 3.

We consider in this model only singly scattered sky radiance, generated by scattering of solar beam radiation along the straight

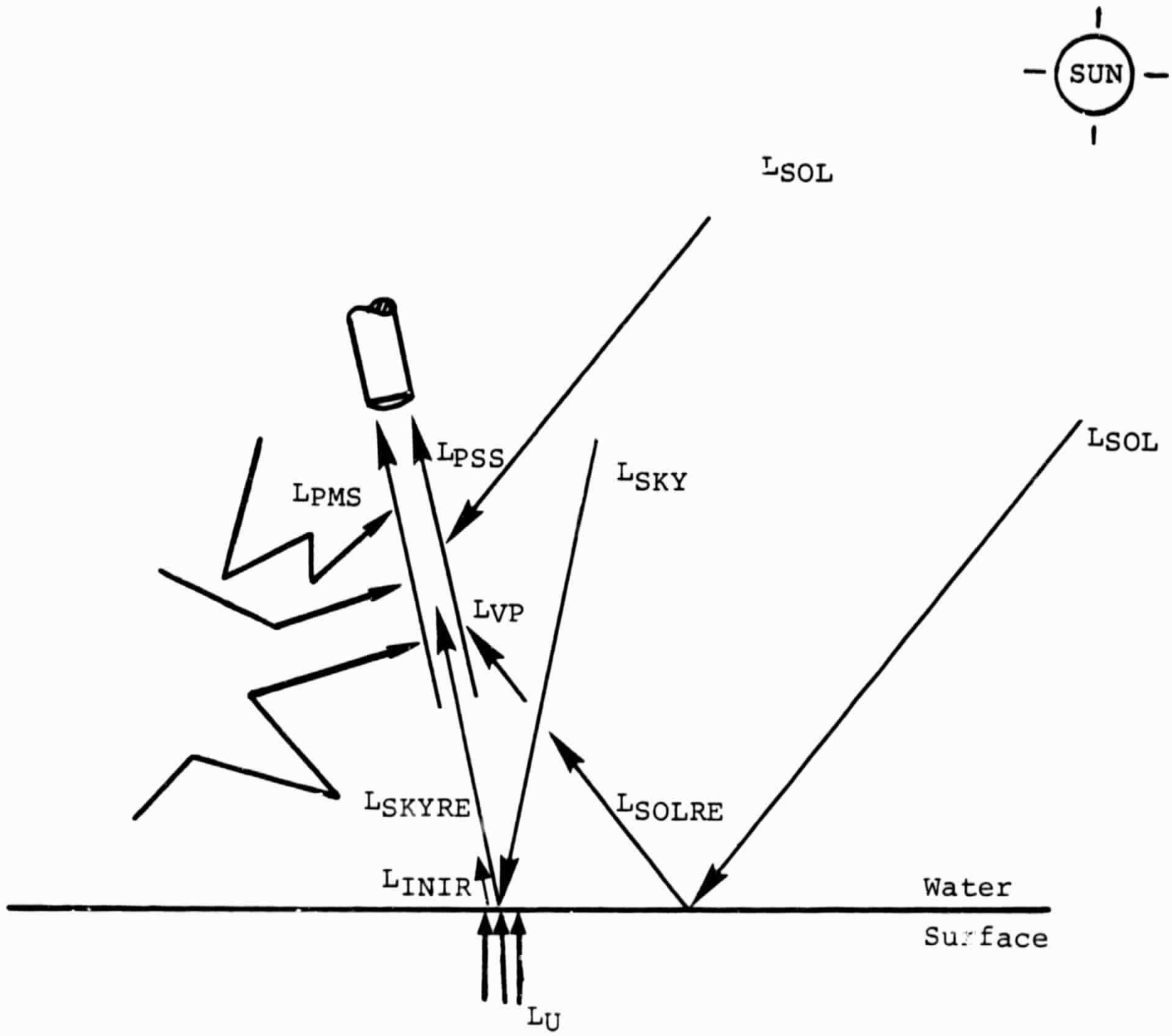

L_{SOL} = direct beam radiance;

L_{PMS} = multiply scattered path radiance;

L_{PSS} = singly scattered path radiance;

L_{SKY} = sky radiance;

L_{SKYRE} = reflected sky radiance;

L_{SOLRE} = reflected solar radiance;

L_U = upward scattered radiance beneath water surface;

L_{INIR} = radiance scattered from beneath water surface.

FIGURE 5. COMPONENTS OF TOTAL RADIANCE DETECTED BY SENSOR

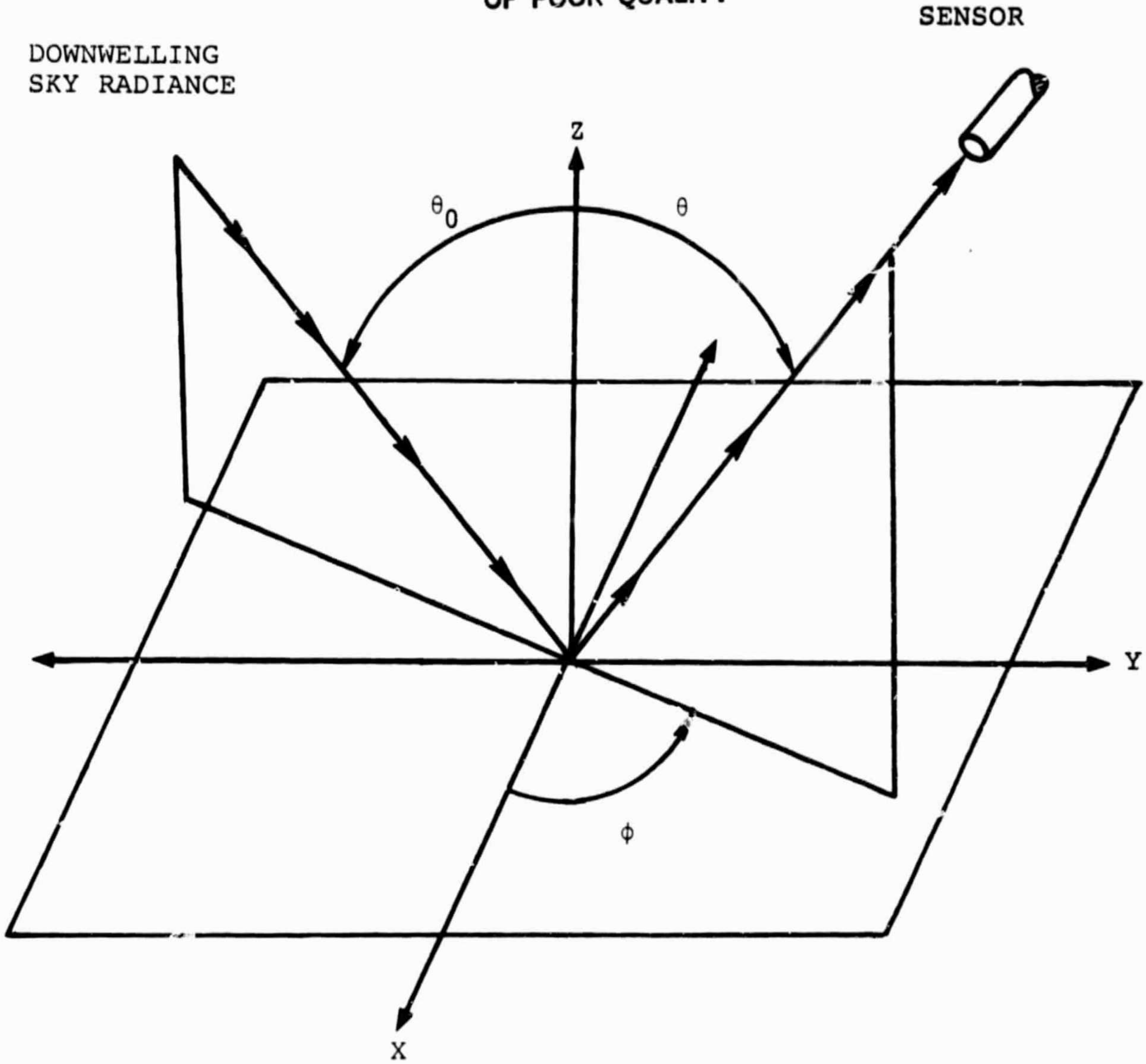

FIGURE 6. GEOMETRY FOR REFLECTED SKY
RADIANCE COMPUTATION.

ORIGINAL PAGE IS
OF POOR QUALITY

line path from the top of the atmosphere to the water surface. In Figure 6, this straight line path has direction $(-\mu,\phi)$, where $\mu = \cos\theta$. In order to define the angle of scattering we must first define two vectors, one defining the direction of a photon leaving the Sun and the other the direction of the singly scattered sky radiation. If $(-\mu_0,\phi_0)$ is the direction of the photon leaving the Sun (where μ_0 is the cosine of the solar zenith angle, θ_0, and ϕ_0 is the photon azimuth), the vector direction of the photon leaving the Sun is

$$\hat{L}_{SOL} = \begin{bmatrix} \sin(\pi-\theta_0)\cos\phi_0 \\ \sin(\pi-\theta_0)\sin\phi_0 \\ \cos(\pi-\theta_0) \end{bmatrix} = \begin{bmatrix} \sqrt{1-\mu_0^2}\ \cos\phi_0 \\ \sqrt{1-\mu_0^2}\ \sin\phi_0 \\ -\mu_0 \end{bmatrix} , \quad (4)$$

and

$$\hat{L}_{SKY} = \begin{bmatrix} \sin(\pi-\theta)\cos\phi \\ \sin(\pi-\theta)\sin\phi \\ \cos(\pi-\theta) \end{bmatrix} = \begin{bmatrix} \sqrt{1-\mu^2}\ \cos\phi \\ \sqrt{1-\mu^2}\ \sin\phi \\ -\mu \end{bmatrix} . \quad (5)$$

The cosine of the scattering angle, χ_{SKY}, is given by the dot product $\hat{L}_{SOL} \cdot \hat{L}_{SKY}$, i.e.

$$\cos\chi_{SKY} = \mu\,\mu_0 + \sqrt{1-\mu^2}\,\sqrt{1-\mu_0^2}\,\cos(\phi-\phi_0) . \quad (6)$$

The equation for singly-scattered sky radiance, L_{SKYSS}, is the well-known formula [14]

$$L_{SKYSS} = \frac{\omega_0 \mu_0 E_0 P(\chi_{SKY})}{4\pi(\mu_0 - \mu)} \left[e^{-\tau_0/\mu_0} - e^{-\tau_0/\mu} \right] \quad (7)$$

where E_0 = solar irradiance at the top of the atmosphere;
ω_0 = atmospheric single scattering albedo;
τ_0 = optical thickness of atmosphere;
$P(\chi_{SKY})$ = scattering phase function for scattering angle χ_{SKY}.

When the sky radiance is reflected off the surface of the water it is diminished by the Fresnel reflectance of the water surface, ρ_F, and further attenuated by the atmosphere on its way to the sensor. Thus, the complete formula for the reflected sky radiance is

$$L_{SKYRE} = \rho_F \, e^{-(\tau_0 - \tau)/\mu} \, L_{SKYSS} \quad (8)$$

where μ is the cosine of the scan angle, τ is the optical depth of the sensor, and $e^{-(\tau_0 - \tau)/\mu}$ is the transmittance of the atmosphere between the water surface and the sensor. At this point we take note of the fact that in the above formula for the singly scattered reflected sky radiance, the reflectance of the water surface and the transmittance of the atmosphere are opposing effects. Assuming the refractive index of water to be 1.33, the

ORIGINAL PAGE IS
OF POOR QUALITY

Fresnel reflectance of water at the nadir view angle reaches a minimum of 0.021 and attains a maximum of 1.0 at the grazing angle. Typical values of ρ_F for angles commonly used in remote sensing range between 2.1 at the nadir to 3.0 at a scan angle of 46^0. The transmittance, on the other hand, reaches a maximum at the nadir and becomes increasingly small as the scan angle increases. These effects will be discussed further in the following chapter.

4.2 SINGLY SCATTERED REFLECTED SOLAR RADIANCE, L_{VP}.

The phenomenon of specular reflection produces an image of the radiation source on the surface of the water. We refer to the image of the Sun on the water surface as the virtual Sun. If the scan plane is coincident with the solar plane and the sensor is scanning on the solar side of the scan plane at a view angle equal to the solar zenith angle, the field of view becomes saturated with the radiance of the Sun's image. Radiance from the virtual Sun is also scattered into the line of sight of the sensor. In the terminology of this report, we refer to singly-scattered path radiance from the Sun as virtual Sun path radiance, L_{VP}.

To find the scattering angle for the computation of singly-scattered virtual Sun path radiance, we note that the zenith angle of a photon leaving the virtual Sun is θ_{SUN} and the azimuth angle is $\phi_0 = \phi_{SUN} + \pi$ (see Figure 7). The vector direction of a photon leaving the virtual Sun is

$$\hat{L}_{VSOL} = \begin{bmatrix} \sin\theta_{SUN} \cos\phi_0 \\ \sin\theta_{SUN} \sin\phi_0 \\ \cos\theta_{SUN} \end{bmatrix} = \begin{bmatrix} \sqrt{1-\mu_0^2} \cos\phi_0 \\ \sqrt{1-\mu_0^2} \sin\phi_0 \\ \mu_0 \end{bmatrix} \qquad (9)$$

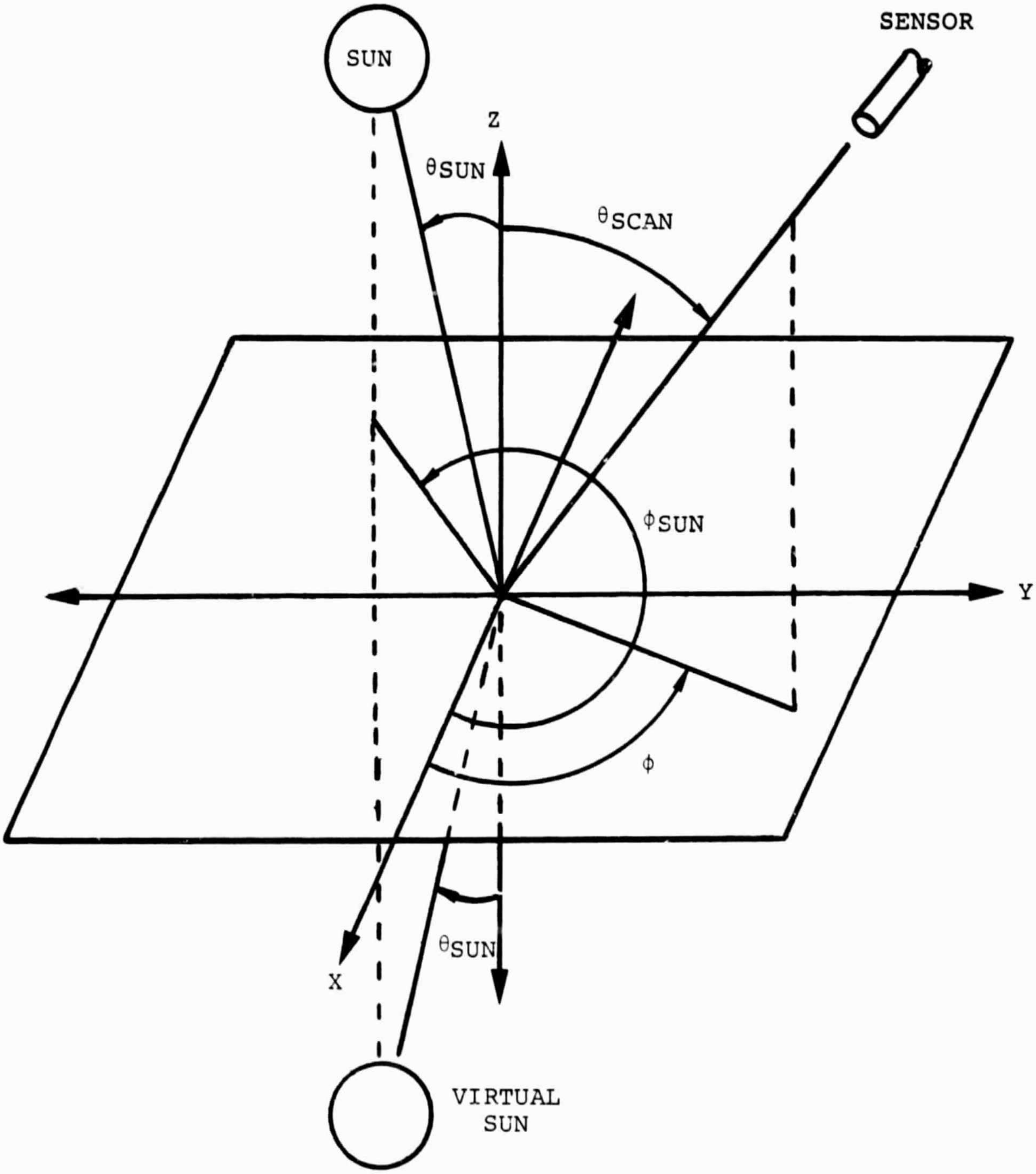

FIGURE 7. GEOMETRY FOR VIRTUAL SUN PATH RADIANCE CALCULATION.

and the vector direction into which photons from the virtual Sun are scattered, creating virtual Sun path radiance is

$$L_{VP} = \begin{bmatrix} \sin\theta\cos\phi \\ \sin\theta\sin\phi \\ \cos\theta \end{bmatrix} = \begin{bmatrix} \sqrt{1-\mu^2}\ \cos\phi \\ \sqrt{1-\mu^2}\ \sin\phi \\ \mu \end{bmatrix} . \qquad (10)$$

The scattering angle is the dot product,

$$L_{VSOL} \cdot L_{VP} = \mu\ \mu_0 + \sqrt{1-\mu^2}\ \sqrt{1-\mu_0{}^2}\ \cos(\phi-\phi_0) . \qquad (11)$$

As in the case of singly scattered sky radiance, the same types of physical interactions which generate singly-scattered sky radiance from direct solar radiation also scatter radiation from the virtual Sun to generate virtual Sun path radiance. Thus, we may use the same equation for singly-scattered sky radiance, with some modifications, to find the singly-scattered virtual Sun path radiance, L_{VP}. One difference is in that the computation of L_{VP} we will now sum the scattered radiation over a path beginning at $\tau = \tau_0$ (the optical depth of the scene viewed by the sensor) and ending at the optical depth of the sensor, τ. If we denote the irradiance of the virtual Sun by $E_o{}'$, we obtain the following formula for singly-scattered path radiance from the virtual Sun:

$$L_{VP} = \frac{\omega_0 \mu_0 E_0' \; p(\cos\chi_{VP})}{4\pi(\mu_0 - \mu)} \left[e^{-(\tau_0-\tau)/\mu_0} - e^{-(\tau_0-\tau)/\mu} \right] . \quad (12)$$

We define E_0' by noting that the E_0' is the image of the Sun reflected in the water surface. Hence, the irradiance of the virtual Sun is the irradiance of the true Sun at the top of the atmosphere attenuated by the atmosphere and the reflectance of the water surface, i.e.,

$$E_0' = \rho_F \, e^{-\tau_0/\mu_0} \, E_0 \quad (13)$$

where ρ_F is the Fresnel reflectance and $e^{-\tau_0/\mu_0}$ is the transmittance of the atmosphere.

4.3 SINGLY SCATTERED PATH RADIANCE, L_{PSS}.

The geometry for singly-scattered path radiance is shown in Figure 8. The formula for singly-scattered path radiance is similar to that for singly-scattered path radiance from the Sun--the same straight line path from τ_0 to τ is used, but E_0 is substituted for E_0' in the formula. The cosine of the scattering angle for singly-scattered path radiance, $\cos\chi_{PSS}$ is also the negative of the cosine of the scattering angle used to compute the phase function for L_{VP}. Thus, $\cos\chi$ is the dot product, $\hat{L}_{SOL} \cdot \hat{L}_{VP}$, vector directions which have already been defined. The formula used to compute singly-scattered solar path radiance is

$$L_{PSS} = \frac{\omega_0 \mu_0 E_0 \; p(\cos\chi_{PSS})}{4\pi(\mu+\mu_0)} \; e^{-\tau_0/\mu_0} \left[e^{(\tau_0-\tau)/\mu_0} - e^{-(\tau_0-\tau)/\mu} \right]$$

(14)

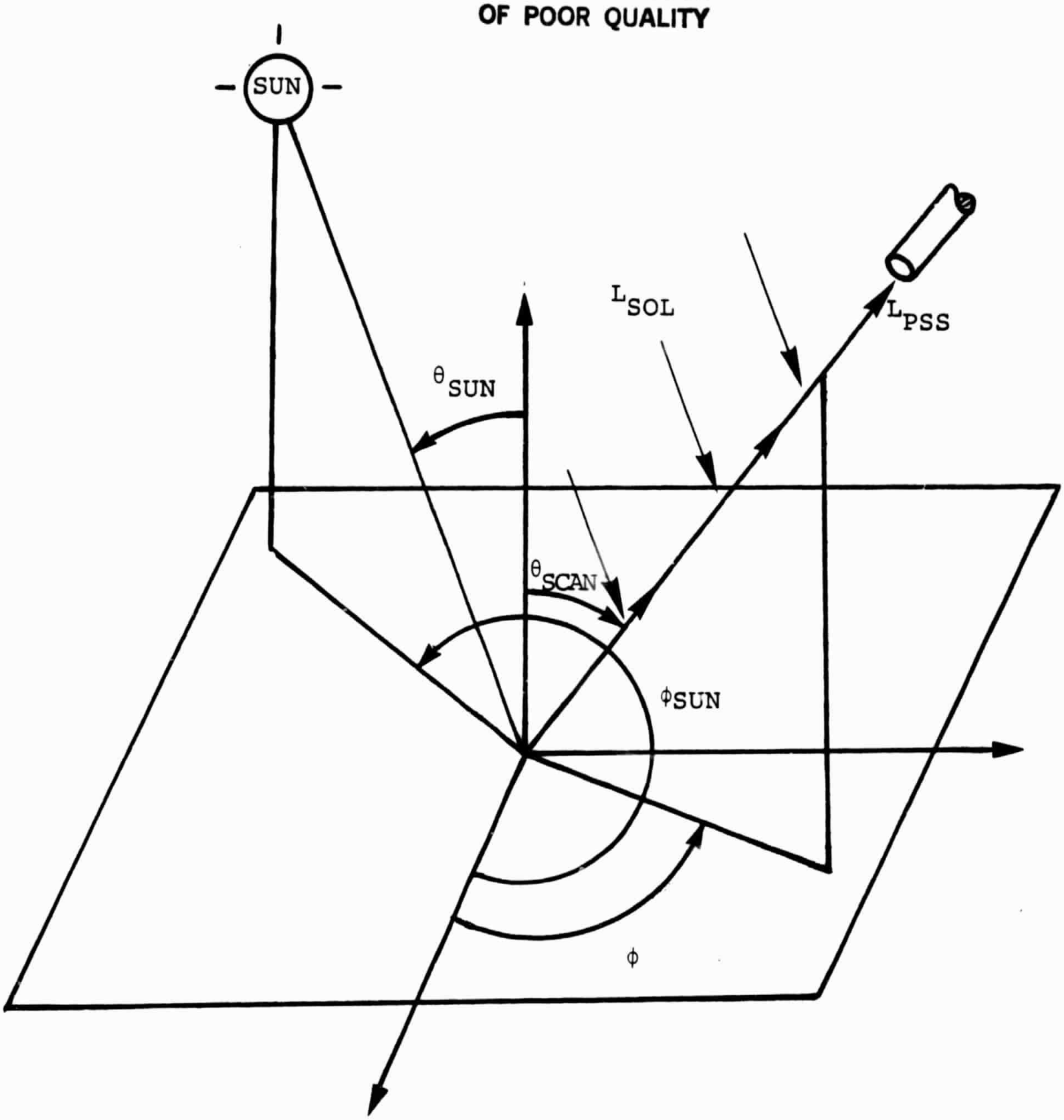

FIGURE 8. GEOMETRY FOR SINGLY SCATTERED PATH RADIANCE, L_{PSS}, CALCULATION.

where the variables in the above equation are as previously defined.

4.4 MULTIPLY SCATTERED PATH RADIANCE, L_{PMS}.

To compute multiply scattered path radiance we use an analytical approximation described in detail in an earlier report [15]. The formula for the computation of L_{PMS} is

$$L_{PMS} = \frac{E_0}{4\pi[\mu_0+(1-\eta)\tau_0]}$$

$$\Bigg(\Big\{(1-\eta)\tau_0[p(\mu,\phi,\mu_0,\pi+\phi_0) + p(\mu,\phi,-\mu_0\phi_0)] + \mu_0 p(\mu,\phi,-\mu_0\phi_0)$$

$$+ \frac{2\mu_0{}^2\rho}{1+2(1-\eta)(1-\rho)\tau_0}\Big\}\left[1-e^{-(\tau_0-\tau)/\mu}\right] + \Big\{(1-\eta)\ p(\mu,\phi,\mu_0,\pi+\phi_0)$$

$$+ p(\mu,\phi,-\mu_0,\phi_0)] - \frac{8(1-\eta)\mu_0{}^2\rho}{1+2(1-\eta)(1-\rho)\tau_0}\Big\}\left[(\tau_0+\mu)e^{-(\tau_0-\tau)/\mu}-(\tau+\mu)\right]\Bigg) \quad (15)$$

The single-scattering phase functions are given by:

$$p(\mu.\phi,\mu_0,\pi+\phi_0) = p\left[\mu\ \mu_0-\sqrt{(1-\mu^2)(1-\mu_0{}^2)}\ \cos(\phi-\phi_0)\right]$$

$$p(\mu,\phi,-\mu_0,\phi_0) = p\left[-\mu\ \mu_0+\sqrt{(1-\mu^2)(1-\mu_0{}^2)}\ \cos(\phi-\phi_0)\right].$$

5
COMPUTER MODEL AND RESULTS

In this chapter we describe implementation of the formulas discussed in Chapter 4 in the computer program called ATCOR. Many of the details of ATCOR have been presented in a previous report [16], so only a brief description of the entire program will be given here. Our discussion will focus primarily on the subroutine ATMSFR, in which the formulas presented in Chapter 4 have been introduced.

5.1 SPECIFICATION OF SOLAR AND SENSOR GEOMETRY

The geometric relationship of the sensor to the environment is shown in Figure 9. The geographic coordinates of the sensor locate the center of a spherical coordinate system used to define angles needed in model calculations. In the diagram the scanner scans along a path from P_1 (the first pixel) to P_n (the last pixel). The azimuth of the scan plane is measured in the counterclockwise direction from north to the first pixel and is read into the program by the routine ATMSFR. The first pixel is always 90° in a clockwise direction from a vector pointing in the direction of the flight.

The solar zenith and azimuth angles are computed automatically once the latitude, longitude, date, time of day (standard time), and zone number are specified. The extraterrestrial solar irradiance is also computed based on these inputs.

5.2 ATMOSPHERIC CORRECTION OPTIONS

Two input parameters set by the user determine which calculations are performed in routine ATMSFR. These parameters are SCATT and OPTION. SCATT may assume the value of either 0 or 1; OPTION can take on the values of 1, 2, or 3. If SCATT is 0, only multiply scattered path radiance is calculated and the value of OPTION can be any integer and will be ignored since only LPMS is then calculated.

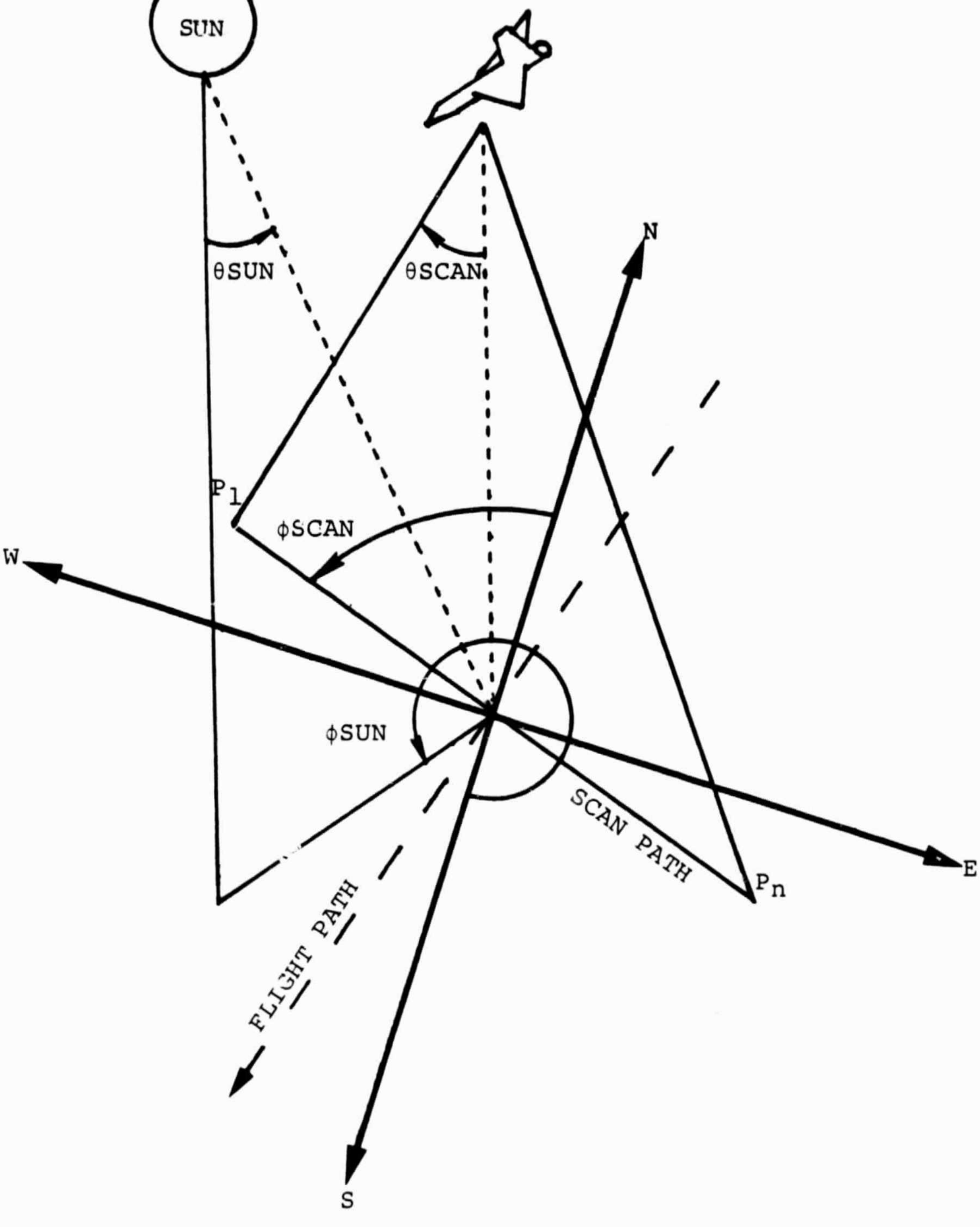

FIGURE 9. SCAN PLANE AND SOLAR GEOMETRY. φSCAN IS MEASURED COUNTERCLOCKWISE FROM NORTH TO PIXEL #1, φSUN IS MEASURED COUNTERCLOCKWISE FROM SOUTH. POSITIVE SCAN ANGLES ARE MEASURED FROM THE FIRST PIXEL TO THE NADIR. NEGATIVE SCAN ANGLES ARE MEASURED FROM THE NADIR TO THE LAST PIXEL. P_1 AND P_n ARE THE FIRST AND LAST PIXELS, RESPECTIVELY.

If SCATT is 1, single scattering computations are performed and the value of OPTION is used to determine which values to calculate. If OPTION = 1, singly scattered path radiance, LPSS, and reflected sky radiance, LSKYRE, are computed. If OPTION = 2, LPSS and virtual sun path radiance, LVP, are computed. If OPTION = 3, LPSS, LSKYRE and LVP are calculated.

OPTION and SCATT are read into the data file on logical unit 4. The format for this record is (5I5), and the variables read in are:

FSTP LSTP PTINC SCATT OPTION

where

FSTP = the number of the first pixel to be processed,
LSTP = the number of the last pixel to be processed,
PTINC = the pixel increment to use in the processing,
and SCATT and OPTION are as previously defined.

The output file which is used by ATMSFR is given in Table 1 and the new subroutine ATMSFR2 is given in Table 2.

5.3 MODEL INPUT PARAMETERS

In addition to the geometric parameters, we must specify parameters characterizing the medium and the measurement system.

The model makes use of several "altitude" values which must be input by the user. First, one must know the actual altitude (km) of the sensor above the surface. Second, one must know the pressure (millibars) of the atmosphere at the surface, and third, one must know the atmospheric pressure (in millibars) at flight altitude. If only the altitudes are known, one can use the tables relating pressure to altitude as given by the U.S. Standard Atmosphere [17].

TABLE 1

INPUT FILE ON LOGICAL UNIT 4

FOR USE BY ATMSFR

ORIGINAL PAGE IS OF POOR QUALITY

LINE NO	READ OCCURS IN ROUTINE	INPUT VARIABLES	FORMAT
1	ATMSFR	FSTP,LSTP,PTINC, SCATT,OPTION	(5I5)
2	DATE	MNTH,DAY,YEAR	(3I4)
3	ANGLES	HOUR,MIN,SEC	(2I5,F6.3)
4	ANGLES	NZ	(I5)
5	ANGLES	LATD,LATM,LATS,LONDG, LONGM,LONGS	(2I5,F6.3,2I5, F6.3)
6	ATMSFR	ZSCAN,ZGRND,LSW	(2F8.5,I5)
7	ATMSFR	(WAVE(I),I=1,QNCHAN)	(10F8.5)
8	ATMSFR	(RHO(I),I=1.QNCHAN)	(10F8.5)
9	PHASE	R,IM	(2F8.6)
10 11-14	PHASE	NWT,NANG,(C(I),I=1,NANG)	(2I5/(10F8.6))
15-79	PHASE	(WTAB(I),(PF(I,J), J=1,NANG),I=1,NWT)	(F10.6/(10 F8.4))
80	RAYLEI	PRESO,PRESZ	(2F10.4)
81	OZONE	NOZ,NPROF,NO3W1,NO3W2	(4I5)
82	OZONE	WAVC1,WAVC2	(2F8.4)
83-153	OZONE	((ZOZ(IZ),O3INT(IZ,IP), IZ=1,NOZ),IP=1,NPROF)	(F7.0, E11.4)
154	OZONE	(O3MAX(IP),IP=1,NPROF)	(10E13.6)
155-169	OZONE	(WAVO3(I),A(I),I=1,NO3W) (NOTE:NO3W=NO3W1 + NO3W2)	(F7.0,E11.4)

TABLE 1 (Cont.)

INPUT FILE ON LOGICAL UNIT 4

FOR USE BY ATMSFR

(CONTINUED)

ORIGINAL PAGE IS
OF POOR QUALITY

LINE NO.	READ OCCURS IN ROUTINE	INPUT VARIABLES	FORMAT
170	OZONE	NOP	(4I5)
171	THICK	NTEX	(I2)
177	THICK	(WAVEX(I),TAUEX(I),I=1,NTEX)	(2F8.4)
178	PARAMS	FSCAT	(10F8.6)
179	AERO	NAER,MPROF,NUZ,MAXG	(5I5)
180	AERO	IPROF	(I5)
181-184	AERO	(WAVAER(I),RIN(I),I=1,NAER)	(10F8.4)
185-230	AERO	((ZUN(IZ),UNIZ(IZ,IP),IZ=1, NUZ),IP=1,MPROF)	(F7.0,E11.4)
231-258	AERO	(X(I),Z(I),I=1,MAXG)	(F7.0,E11.4)
259	ATMSFR	PHID,PHIM,PHIS	(2I3,F6.3)
		$ENDFILE	

TABLE 2

PROGRAM LISTING

```
C                                         ATMSFR2
C****************************************************************************
C****************************************************************************
C****************************************************************************
C****************************************************************************
C****************************************************************************
C   THIS IS A MODIFIED VERSION OF THE ROUTINE "ATMSFR" TO BE USED TO
C  CORRECT FOR ATMOSPHERIC EFFECTS UNIQUE TO LARGE BODIES OF WATER. IT
C  WILL PERFORM IDENTICALLY AS ITS PREVIOUS VERSIONS WHEN THE VALUE ZERO
C  ( OR BLANKS )  ARE READ INTO THE INTEGER VARIABLE "SCATT." THUS ANY
C  PREVIOUS DATA SET MAY BE USED WITH THIS ROUTINE TO PRODUCE THE SAME
C  MULTIPLY SCATTERED PATH RADIANCE CORRECTIONS.
C   WHEN SCATT=1, HOWEVER, ATMSFR2 WILL CALCULATE ONLY SINGLY SCATTERED
C  QUANTITIES. ANOTHER NEW VARIABLE, "OPTION," IS READ IN. WHEN SCATT=O
C  OPTION HAS NO EFFECT. WHEN SCATT=1, OPTION CHOOSES WHICH RADIANCE
C  CONTRIBUTIONS TO CORRECT FOR.
C   IF OPTION=O, ONLY THE PATH RADIANCE PRODUCED BY THE DIRECT SOLAR
C  RADIATION IS SUBTRACTED FROM THE EXPERIMENTAL RADIANCES. IF OPTION=1,
C  BOTH THE DIRECT PATH RADIANCE AND THE SKY RADIANCE SPECULARLY RE-
C  FLECTED FROM THE WATER SURFACE INTO THE SENSOR ARE SUBTRACTED. WHEN
C  OPTION=2, THE DIRECT PATH RADIANCE AS WELL AS THE PATH RADIANCE PRO-
C  DUCED BY THE SPECULARLY REFLECTED VIRTUAL IMAGE ( I.E. THE "MIRROR
C  IMAGE" ) OF THE SUN FROM THE WATER IS SUBTRACTED. WHEN OPTION=3, ALL
C  THREE QUANTITIES ARE SUBTRACTED. ATMSFR2 CALLS ALL AND ONLY THE SAME
C  ROUTINES AS ITS PREDECESSOR VERSIONS AND IS CALLED IN THE SAME MANNER.
C  WE DEFINE THE FOLLOWING VARIABLES:
C
C  LPATH - PATH RADIANCE GENERATED BY THE DIRECT SOLAR RADIATION.
C
C  LRSKY - REFLECTED SKY RADIANCE OBSERVED AT SENSOR.
C
C  LVIRP - PATH RADIANCE GENERATED BY THE VIRTUAL IMAGE OF THE SUN OB-
C                 SERVED AT THE SENSOR.
C
C                               MODIFICATIONS PROGRAMMED BY JIM LIERZER
C                                                          JAN. 5, 1982
C
      INTEGER FUNCTION ATMSFR(L,CONTRL,MCHAN,MSS)
C *==========================================================================
C ========*
C *--------------------------------------------------------------------------
C --------*
C *VERSION 11LINE/QLINE COMMON BLOCKS VER.NA3.2 15AUG77 RHH--NASA UNIVAC
C  VERSION*
C *         VER.3.0   14APR77 -- 200/24 CHANNEL VERSION ALL PUT TOGETHER
C          *
C *         VER.3.0A   6JUN77 -- FINISH MAKING FORTRAN COMPATIBLE, QBREAL
C SWITCH   *
C *         VER.3.0B   7JUN77 -- QBANG, QDANG
C          *
C *         VER.3.0C 10JUN77 -- JM'S QANCIL, QIOPAR COMMON BLOCKS ADDED
C          *
C *         VER.3.0D 30JUN77 -- QIBSQL;  /QANCIL/ IN ALL ROUTINES
C          *
C *         VER.3.2   12AUG77 -- MOO2, NOT 1,0; QPOLY; QM1,2; Q..999;
C QBSEQL, ETC.*
C *         VER.NA3.2  15AUG77--DIMENSIONS FOR NASA-LEWIS UNIVAC
C          *
C           VER.NA3.3 5JAN82 -- ADDED SINGLE SCATTER, LPATH, LRSKY, LVIRP
C          *
```

TABLE 2 (Cont.)

```
C *----------------------------------------------------------------------
C --------*
C *MAIN COMMON BLOCK FOR USE BY MONITOR, INPUT FSR, MODULES, AND OUTPUT
C FSR
      COMMON /QCOM/ QCVERS(4),QNSAS(6),QNSS,QLINE,QSLINE,
     2          QSTEP,QMCHAN,QMSS,QNCHAN,QNDACH,QFILE,
     3          QBNONE,QBEND,QBPAS1,QBPOLY,QBTRSE,QFLDID(24),QSPARE(93),
     4          QBLSEG,QB6EQ8,QBSEQL,QBANG,QDANG,QBREAL,QBFACT,
     5          QTITLE(120),QTITL2(120),QLIST(6,20),QSCHAN(200),
     6          QFACTN(200),QFACTA(200),QCM999
      REAL      QFACTM,QFACTA,QBANG,QDANG
      INTEGER   QCVERS,QLINE,QSLINE,QNSAS,QNSA,QNSB,QKS,QNA,QNB,QKP,QNSS
      INTEGER   QFRSTL,QLASTL,QSTEPL,QFRSTP,QLASTP,QSTEPP
      INTEGER   QSTEP,QMCHAN,QMSS,QNCHAN,QNDACH,QFILE,QSPARE,QSCHAN
      LOGICAL   QBNONE,QBEND,QBPAS1,QBPOLY,QBLSEG,QBTRSE,QBSEQL
      LOGICAL   QFLDID,QTITLE,QTITL2,QLIST
      EQUIVALENCE (QNSAS(1),QFRSTL,QNSA), (QNSAS(2),QLASTL,QNSB)
      EQUIVALENCE (QNSAS(3),QSTEPL,QKS),  (QNSAS(4),QFRSTP,QNA)
      EQUIVALENCE (QNSAS(5),QLASTP,QNB),  (QNSAS(6),QSTEPP,QKP)
      LOGICAL   QCM000,QCM999
      EQUIVALENCE (QCM000,QCVERS)
C *----------------------------------------------------------------------
C --------*
C*ANCILLARY DATA COMMON BLOCK
      COMMON /QANCIL/ QHDNUM,QAHEAD(200),QNCIL(180),QAN999
      INTEGER   QHDNUM,QAHEAD,QNCIL
      LOGICAL   QAN000,QAN999
      EQUIVALENCE (QAN000,QHDNUM)
C *----------------------------------------------------------------------
C --------*
C**PARAMETERS* FOR USE IN FORTRAN PROGRAMS
      INTEGER   QOCHAN,QOCHN2,QONSS,QONSS2,QOIBUF,QOOBUF
      INTEGER   QODILN,QOMX2 ,QOMX4 ,QOLDTA,QOLDT2,QOLCTL
      INTEGER   QUDATA,QURTRY,QUPRNT,QUERR ,QUPNCH,QUPRNT,QUMAP
      INTEGER   QOVRTX,QONREG,QONSEG
      INTEGER   QOCVER(4)
C*PARAMETERS -- DECLARATION SIZES FOR DATA ARRAYS
      DATA QOCHAN/200/
      DATA QOCHN2/24/
      DATA QONSS /3264/
      DATA QONSS2/824/
      DATA QOIBUF/22293/
      DATA QOOBUF/22293/
      DATA QOVRTX/101/
      DATA QONREG/24/
      DATA QONSEG/24/
C*PARAMETERS -- MACHINE DEPENDENT LENGTH ATTRIBUTES, ETC.
      DATA QODILN/4/
      DATA QOMX2 /2/
      DATA QOMX4 /4/
      DATA QOLDTA/4/
      DATA QOLDT2/4/
      DATA QOLCTL/4/
C*PARAMETERS -- STANDARD I/O UNITS
      DATA QUDATA/4/
      DATA QURTRY/5/
      DATA QUPRNT/6/
      DATA QUERR /6/
      DATA QUPNCH/7/
      DATA QUPRNT/8/
```

ORIGINAL PAGE IS
OF POOR QUALITY

TABLE 2 (Cont.)

```
      DATA QUMAP /9/
C *PARAMETERS -- COMMON BLOCK VERSION TO CHECK THAT ALL MODULES COMPILED
C  TO MATCH
      DATA QOCVER/'VNA3','MOO2','77/0','8/15'/
C *---------------------------------------------------------------------
C ---------*
C *=====================================================================
C ========*
      INTEGER  VERMES(14)
C
C   WHEREVER "10" APPEARS IN THE FOLLOWING DECLARATIONS, IT CAN BE
C      REPLACED BY THE NUMBER OF CHANNELS. WHEREVER "344" APPEARS, IT
C      MEANS NUMBER OF POINTS.
C
      REAL L(MCHAN,MSS),MUO,MUOSQ,NU,MU,MUSQ,MFACT,EFACT(10,344),LPATH(1
     10,344)
      REAL OM(10), ETA(10), A(10), B(10), SIG(10), LAMPP(10), PHIP(10),
     1     AT(10), BT(10), ATP(10), BTP(10), BTPP(10), CTPP(10),DTPP(10),
     2     EO(10), E(10),  FE(10),  FP(10),  TAU(10), RHO(10), ALPHA(10),
     3     G(10),   TAUZ(10),MUSQ(10),LBEAM(10),LSURF(10),FSCAT(10),
     4     RHOS(10),LINTR(10),ATPP(10),D(10),WAVE(10),TAS(10)
     5     ,TA(10),TR(10),TAUO3(10),TAUZO3(10),TAZ(10),TRZ(10)
      INTEGER PHID,PHIM,FSTP,LSTP,PTINC,SCATT
      INTEGER OPTION
      REAL FRES(344),LRSKY(10,344),LVIRP(10,344)
      REAL ED(10)
      REAL INDEX,THETTA,REFRAC,AX,BX,SINA,SINB,TANA,TANB,FRESUN,FRESO,
     1      EFACTO,EFACTS,CONST,EXPO1,EXPO2,COND,COND1,COND2,COND3,
     2      ARGSKY,ARGVIR,PFSKY,PFVIR,MUFAC1,MUFAC2,ETOTF
C
C       INDEX=REFRACTIVE INDEX OF THE LAKE WATER. WE SET INDEX=1.33, THE
C         REFRACTIVE INDEX FOR PURE WATER, BUT YOU MAY WISH TO REPLACE
C         THIS WITH EMPIRICAL VALUES.
C       FRESO=THE LIMITING CASE OF THE FRESNEL REFLECTANCE AT ZERO ANGLE
C         OF INCIDENCE. THIS WILL VARY WITH "INDEX."
C       WHEN MU APPROACHES MUO OR TAU(I) APPROACHES TAUZ(I), THE STAN-
C         DARD SINGLE SCATTERING RADIANCE FORMULAS TRUNCATE MOST OR ALL
C         OF THE SIGNIFICANT FIGURES, AND THE EXPONENTIALS IN THEM MUST
C         BE EXPANDED. "COND" CONTAINS THE VALUE TO CHECK AGAINST TO DE-
C         CIDE WHEN TO USE THE EXPANSIONS. SET COND=10**(N-M) WHERE N=
C         NUMBER OF SIGNIFICANT FIGURES DESIRED, M=MAXIMUM NUMBER OF FI-
C         GURES HELD BY THE MACHINE. WE TAKE COND=0.01. IN REAL*4 PRE-
C         CISION AND EXPANSIONS TO FOURTH ORDER TERMS, THIS WILL GUARAN-
C         TEE RADIANCES TO AT LEAST THREE SIGNIFICANT FIGURES.
C
      DATA INDEX/1.33/,FRESO/0.0200593122/,COND/0.01/
      INTEGER CONTRL(MSS)
      DATA PRIOR/0./
C*********************************************************************
      DATA VERMES/'ATMS','FR: ','TURN','ER A','TMOS','PHER','IC M','ODEL
     1',' RE','T/SH','W VO','.0 6','/16/','77*'/
      DATA OML/.9999/
      DATA EPS/0.001/,PI/3.141592654/
C
C   THESE "DATA" STATEMENTS ARE FOR DEBUGGING ONLY.
C
C      DATA WAVE/ .428, .466, .508, .549, .592, .632, .674, .714, .756,
C .794/
C     DATA LSW/6/
C     DATA Z/12.323/
```

TABLE 2 (Cont.)

```
C      DATA RHO/.02,.02,.02,.02,.02,.02,.02,.02,.02,.02/
C
C
C   NOTE THAT WHEN YOU ENCOUNTER THE CALLS TO FUNCTION PF, VIZ.
C         PF(ARGUMENT,I,TR(I),TAS(I))
C  THE FOURTH ARGUMENT SHOULD BE TAS(I), NOT TA(I), WHERE
C         TAS(I)=FSCAT(I)*TA(I)
C  SO THAT TAS(I) IS THE AEROSOL OPTICAL THICKNESS DUE ONLY TO SCAT-
C  TERING.
C
      CON = 7.9577472E-02
      ATMSFR = 0
      CALL QQCALD(PRIOR,DATA,CONTRL,QMCHAN,QMSS)
      IF (QBNONE.OR.QBPAS1)RETURN
      GO TO (1,99,3,99,99,6,99,8,99,99,99), QSTEP
99    RETURN
C***************************************************************
C  QSTEP=1 -- CONSTRUCT QLINE LINKAGE TO PRIOR MODULE SUPPLYING DATA:
C***************************************************************
 1    PRIOR = L(1,1)
      RETURN
C***************************************************************
C   QSTEP=3 -- INITIALIZE;  PRINT MODULE IDENTIFICATION, READ CONTROL
C DATA:
C***************************************************************
 3    CONTINUE
C   CALL QQVERS TO PRINT MODULE NAME, DESCRIPTION, VERSION, DATE,
C PROGRAMMER,
C  AND TO CHECK THAT THE COMMON BLOCK VERSION "QQCVER" IS CURRENT
C     CALL QQVERS(VERMES,QQCVER)
C  DON'T FORGET TO REMOVE THE "C" IN COLUMN 1 OF THE ABOVE COMMENT WHEN
C         INTERFACING WITH "ATCOR."
C  I HAVE DELETED THE CALL TO QQVERS IN ORDER TO RUN ATMSFR
C  ALONE FOR DEBUGGING PURPOSES.     JIM LIERZER
      WRITE (QUPRNT,100)
  100 FORMAT('OATMSFR:  ENTER FIRST PIXEL, LAST PIXEL, PIXEL INCREMENT,'
     1      ,' SCATT, AND OPTION (5I5)')
      WRITE(QUPRNT,101)
  101 FORMAT('    WHERE SCATT=0 FOR MULTISCATTERING,'
     1      /'           SCATT=1 FOR SINGLE SCATTERING,'
     2      /'           OPTION=0 FOR LPATH ONLY,'
     3      /'           OPTION=1 FOR LPATH+LRSKY,'
     4      /'           OPTION=2 FOR LPATH+LVIRP,'
     5      /'           OPTION=3 FOR LPATH+LRSKY+LVIRP.')
      READ(QUDATA,105)FSTP,LSTP,PTINC,SCATT,OPTION
  105 FORMAT(5I5)
      RETURN
C***************************************************************
C   QSTEP=6 -- BEGINNING OF REGION:
C***************************************************************
 6    CONTINUE
C
C    COMPUTE WAVELENGTH DEPENDENT CONSTANTS
C
      CALL DATE(QUDATA,QUPRNT, NDAY)
      CALL ANGLES(QUDATA,QUPRNT,NDAY, PHIO,THETAO)
C     READ HEIGHT OF SCANNER, HEIGHT OF GROUND, PRINT/WRITE TAPE SWITCH
      READ(QUDATA,263) ZSCAN,ZGRND,LSW
 263  FORMAT(2F8.5,I5)
      ZSC=ZSCAN*3280.833
```

ORIGINAL PAGE IS
OF POOR QUALITY

TABLE 2 (Cont.)

```
      WRITE(QUPRNT,253)ZSC
  253 FORMAT(' ',19X,'SENSOR ALTITUDE',F10.1,' FEET')
      Z = ZSCAN-ZGRND
C     READ SCANNER WAVELENGTHS, ESTIMATED BACKGROUND REFLECTANCES
      READ (QUDATA,264) (WAVE(I),I=1,QNCHAN)
      READ (QUDATA,264) (RHO(I),I=1,QNCHAN)
 264  FORMAT(10F8.5)
      CALL PHASE(QUDATA,QUPRNT,QNCHAN,WAVE)
      CALL RAYLEI(QUDATA,QNCHAN,WAVE, TR,TRZ)
      CALL OZONE(QUDATA,QUPRNT,QNCHAN,WAVE,Z, TAUO3,TAUZO3)
      CALL THICK(QUDATA,QUPRNT,QNCHAN,WAVE, TAU)
      CALL PARAMS(QUDATA,QUPRNT,TR,TAUO3,TAU,QNCHAN, ETA,OM,TAS,FSCAT)
      CALL AERO(QUDATA,QUPRNT,QNCHAN,WAVE,Z,TAU,TR,TAUO3, TAZ,TA)
      MUO = COS(THETAO)
      CO2 = 2.*MUO
      MUOSQ = MUO*MUO
      CALL SOLAR(WAVE,QNCHAN,NDAY,EO)
C
C     CALCULATE ANGULAR QUANTITIES (DEPENDENT ON AZIMUTH ANGLE ONLY)
C
C     READ THE AZIMUTH ANGLE COUNTERCLOCKWISE FROM NORTH TO ( THE FIRST
C          PIXEL OF THE ) SCAN PLANE.
      READ (QUDATA,265) PHID,PHIM,PHIS
      WRITE (QUPRNT,270) PHID,PHIM,PHIS
  270 FORMAT('O',19X,'AZIMUTH ANGLE MEASURED COUNTERCLOCKWISE FROM NORT'
     1       ,'H TO FIRST PIXEL'/' ',28X,'OF SCAN PLANE IS ',I3,
     2       ' DEGREES,',I3,' MINUTES,',F5.1,' SECONDS.')
 265  FORMAT(2I3,F6.3)
      PHI = 1.7453293E-02*PHID + 2.9088821E-04*PHIM + 4.8481368E-06*PHIS
      FPH = SQRT(1.0 - MUO*MUO)*COS(PHI-PHIO)
      IF (SCATT.EQ.O.OR.OPTION.LT.2) GO TO 301
C
C     FIND THE FRESNEL REFLECTANCE OF THE DIRECT SOLAR RADIATION
C         WHENEVER LVIRP IS DESIRED.
C
      IF (THETAO)39,43,39
   39 THETTA=ABS(THETAO)
      REFRAC=APSIN(SIN(THETTA)*1./INDEX)
      AX=THETTA-REFRAC
      BX=THETTA+REFRAC
      SINA=SIN(AX)
      SINB=SIN(BX)
      TANA=TAN(AX)
      TANB=TAN(BX)
      FRESUN=0.5*((SINA*SINA)/(SINB*SINB)+(TANA*TANA)/(TANB*TANB))
      GO TO 299
   43 FRESUN=FRESO
  299 WRITE(QUPRNT,300)FRESUN
  300 FORMAT(' ',19X,'THE FRESNEL REFLECTANCE FOR THE DIRECT SOLAR ',
     1                'RADIATION IS',F10.5)
  301 CONTINUE
C
C     ECHO A LOT OF DATA TO TELL THE USER THE INPUT DATA WHICH GIVE
C       HIM THE REST OF THE NUMBERS.
C
      WRITE(QUPRNT,561)LSW,SCATT,OPTION
  561 FORMAT(' ',10X,'SWITCH POSITION',3X,I1,5X,'SCATTERING MODE',3X,I1,
     1       5X,'OPTION',3X,I1)
      WRITE(QUPRNT,30)
   30 FORMAT('O',10X,'ALL RADIANCES ARE IN UNITS OF MILLIWATTS PER CEN',
```

TABLE 2 (Cont.)

```
     1 'TIMETER SQUARED'/' ',14X,'PER MICROMETER PER STERADIAN.'/
     2  11X,'ALL IRRADIANCES ARE IN UNITS OF MILLIWATTS PER CENTIMETER'
     3     ,' SQUARED'/15X,'PER MICROMETER.'/
     4  11X,'ALL WAVELENGTHS ARE IN MICROMETERS.')
      IF (SCATT.EQ.O) GO TO 36
      WRITE(QUPRNT,31)
   31 FORMAT(' ',10X,'WE SHALL CALCULATE SINGLY SCATTERED RADIANCES ',
     1                'ONLY.')
      IF (OPTION.EQ.O) WRITE(QUPRNT,32)
   32 FORMAT(' ',10X,'ONLY THE DIRECT PATH RADIANCE WILL BE CONSIDERED.'
     1      )
      IF (OPTION.EQ.1) WRITE(QUPRNT,33)
   33 FORMAT(' ',10X,'THE DIRECT PATH RADIANCE AND THE REFLECTED SKY ',
     1                'RADIANCE WILL BE CONSIDERED.')
      IF (OPTION.EQ.2) WRITE(QUPRNT,34)
   34 FORMAT(' ',10X,'THE DIRECT PATH RADIANCE AND THE VIRTUAL PATH ',
     1                'RADIANCE WILL BE CONSIDERED.')
      IF (OPTION.EQ.3) WRITE(QUPRNT,35)
   35 FORMAT(' ',10X,'THE DIRECT PATH RADIANCE AND BOTH THE VIRTUAL ',
     1                'PATH RADIANCE AND THE REFLECTED SKY RADIANCE ',
     2                'WILL BE CONSIDERED.')
      GO TO 38
   36 WRITE(QUPRNT,37)
   37 FORMAT(' ',10X,'WE SHALL CALCULATE MULTIPLY SCATTERED RADIANCES ',
     1                'ONLY.')
   38 CONTINUE
      WRITE(QUPRNT,275) QBANG,QDANG
  275 FORMAT(20X,'MAXIMUM SCAN ANGLE=',F9.7,' RADIANS.         ANGULAR RE
     1SOLUTION OF SCANNER IS ',F9.7,' RADIANS.')
      WRITE(QUPRNT,276)(I,I=1,QNCHAN)
276   FORMAT('1 CHANNEL             ',10I10)
      WRITE(QUPRNT,277)(WAVE(I),I=1,QNCHAN)
277   FORMAT('- WAVELENGTH            ',10F10.5)
      WRITE(QUPRNT,279)(TAU(I),I=1,QNCHAN)
279   FORMAT('- INTERPOLATED OPTICAL',10F10.5)
      WRITE(QUPRNT,280)
  280 FORMAT('          THICKNESS')
      WRITE(QUPRNT,281)(RHO(I),I=1,QNCHAN)
281   FORMAT('- BACKGROUND ALBEDO    ',10F10.5)
      WRITE(QUPRNT,283)(OM(I),I=1,QNCHAN)
283   FORMAT('- SINGLE SCATTERING    ',10F10.5)
      WRITE(QUPRNT,284)
  284 FORMAT('          ALBEDO')
      WRITE(QUPRNT,285)(FSCAT(I),I=1,QNCHAN)
285   FORMAT('- SCATTERING PARAMETER',10F10.5)
      WRITE(QUPRNT,287)
  287 FORMAT('            (FSCAT)')
      WRITE(QUPRNT,290)(TAUO3(I),I=1,QNCHAN)
  290 FORMAT('- OZONE OPTICAL',7X,10F10.5)
      WRITE(QUPRNT,292)
  292 FORMAT('        THICKNESS')
      WRITE(QUPRNT,295)(TR(I),I=1,QNCHAN)
  295 FORMAT('- RAYLEIGH OPTICAL',4X,10F10.5)
      WRITE(QUPRNT,296)
  296 FORMAT('            THICKNESS')
      DO 10 I=1,QNCHAN
         TAUZ(I) = TAUZO3(I) + TRZ(I) + TAZ(I)
           IF (SCATT.EQ.O) GO TO 500
C
C          COMPUTE WAVELENGTH DEPENDENT QUANTITIES NEEDED FOR
```

ORIGINAL PAGE IS
OF POOR QUALITY

TABLE 2 (Cont.)

```
C          SINGLE SCATTERING CALCULATIONS
C
           SIG(I) = TAU(I) - TAUZ(I)
           EFACTO = EXP(SIG(I)/MUO)
           CONST = CON*OM(I)*EO(I)
           EFACTS = EXP(-TAU(I)/MUO)
           ETOTF = (1.-ETA(I))*TAU(I)
           E(I) = (MUO*MUO*EO(I)/(MUO+ETOTF))*(1+(2.*RHO(I)*ETOTF)/
     1                                        (1.+2.*ETOTF))
           FE(I)=MUO*EO(I)/E(I)
C         COMPUTE DIRECT IRRADIANCE AT SURFACE
           ED(I)=MUO*EO(I)*EFACTS
           GO TO 15
  500      CONTINUE
C
C          COMPUTE WAVELENGTH DEPENDENT QUANTITIES NEEDED FOR
C          MULTI SCATTERING CALCULATIONS
C
         IF (OM(I).GT. OML) GO TO 20
           A(I) = OM(I)* (1.0-ETA(I))
           B(I) = 1.0 + A(I) - OM(I)
           C = A(I) + B(I)
           NU = MUO / SQRT(C*(B(I)-A(I)))
           NUSQ(I) = NU*NU
           SIG(I) = TAU(I) - TAUZ(I)
           ARG1 = SIG(I)/NU
           SH1 = SINH(ARG1)
           CH1 = COSH(ARG1)
           ARG2 = TAU(I)/NU
           SH2 = SINH(ARG2)
           CH2 = COSH(ARG2)
           ARG3 = CO2*ARG2
           SH3 = SINH(ARG3)
           CH3 = COSH(ARG3)
           ARG4 = ARG3*TAUZ(I)/TAU(I)
           SH4 = SINH(ARG4)
           CH4 = COSH(ARG4)
C          COMPUTE LAMBDA DOUBLE PRIME
           LAMPP(I) = CON*NUSQ(I) * OM(I)*EO(I) /(B(I)*NU*SH2 + MUO*CH2)
C          COMPUTE PHI PRIME
           PHIP(I) = 2.0*RHO(I)*MUOSQ*LAMPP(I)/
     1     (MUO*CH3+NU*(B(I)-A(I)*RHO(I))*SH3)
C          COMPUTE OTHER CONSTANTS
           AT(I) = NU*SH1
           BT(I) = CH1
           ATP(I) = B(I)*NU*SH1 + MUO*CH1
           BTP(I) = B(I)*CH1 + MUO*SH1/NU
           ATPP(I) = C*NU*SH4 + MUO*CH4
           BTPP(I) = 2.0*C*((1.0-OM(I))*NU*SH4 + MUO*CH4)
           CTPP(I) = C*NU*SH3 + MUO*CH3
           DTPP(I) = 2.0*C* ((1.0-OM(I))*NU*SH3 + MUO*CH3)
C          COMPUTE TOTAL IRRADIANCE AT SURFACE
           E(I) = 6.28318531*PHIP(I) * (NU*B(I)*SH3 +MUO*CH3)/
     1     (NUSQ(I)*OM(I)*RHO(I))
           FE(I) = MUO*EO(I)/E(I)
C          COMPUTE DIRECT IRRADIANCE AT SURFACE
           ED(I)=MUO*EO(I)*EXP(-TAU(I)/MUO)
           GO TO 15
C        CALCULATE SIMILAR CONSTANTS FOR OMEGA=1
   20    CONTINUE
```

TABLE 2 (Cont.)

```
            SF = 1.0-ETA(I)
            D(I) = MUO/SF
            FP(I) = CON*SF*EO(I) / (MUO + SF*TAU(I))
            CHI = CO2*MUO*RHO(I) / (1.0 + 2.0*SF*(1.0-RHO(I))*TAU(I))
            ALPHA(I) = CHI* (4.0 + 1.0/SF)
            G(I) = 4.0*CHI
            SIG(I) = TAU(I) - TAUZ(I)
C           COMPUTE TOTAL IRRADIANCE AT SURFACE
            E(I) = 6.28318531*CHI*FP(I)*(1.0 + 2.0*SF*TAU(I))/(RHO(I)*SF)
            FE(I) = MUO*EO(I)/E(I)
C           COMPUTE DIRECT IRRADIANCE AT SURFACE
            ED(I) = MUO*EO(I)*EXP(-TAU(I)/MUO)
   15     CONTINUE
C
C       NOW CALCULATE THOSE QUANTITIES WHICH ARE DEPENDENT ON SCAN ANGLE.
C
          DO 2019 IP=FSTP,LSTP,PTINC
            THETA = QBANG - (IP-1)*QDANG
            FPHI = FPH
            IF (THETA .LE. 0.0) FPHI = -FPH
            MU = COS(THETA)
            FMU = MU*MUO
            MUSQ = MU*MU
            ROOT = SQRT(1.0-MUSQ)
C
C  THE FOLLOWING EQUATION FOR ARG IS CORRECT. REMEMBER THAT PHIO
C  IN THIS PROGRAM REPRESENTS THE SOLAR AZIMUTH ANGLE WHILE IN THE
C  LITERATURE PHIO USUALLY REPRESENTS THE AZIMUTH ANGLE OF THE DIR-
C  ECTION OF THE SOLAR RADIATION. THE TWO ANGLES ARE SHIFTED BY 90
C  DEGREES, CAUSING FPHI TO CHANGE SIGN.
C
            ARG = FMU +FPHI*ROOT
            IF (SCATT.EQ.0) GO TO 510
C
C           BLOCK OF COMPUTATIONS FOR SINGLY SCATTERED RADIANCES.
C           THESE QUANTITIES DEPEND ON SCAN ANGLE.
C
            PF2=PF(-ARG,I,TR(I),TAS(I))
            EXPO1=SIG(I)/MU
            EFACT(I,IP)=EXP(-EXPO1)
            MUFAC1=(MU+MUO)/MUO
            COND1=EXPO1*MUFAC1
            IF (ABS(COND1).LT.COND) GO TO 501
C
C           CALCULATE SINGLY SCATTERED PATH RADIANCE
C
            LPATH(I,IP)=(CONST/MUFAC1)*PF2*EFACTS*(EFACTO-EFACT(I,IP))
            GO TO 502
C
C           EITHER MUO AND -MU OR TAU(I) AND TAUZ(I) ARE TOO CLOSE TO-
C           GETHER, SO WE MUST EXPAND THE EXPONENTIALS IN THE PATH RADI-
C           ANCE FORMULA TO FOURTH ORDER TERMS AND CANCEL TERMS.
C
  501       LPATH(I,IP)=CONST*PF2*EFACTS*EFACT(I,IP)*EXPO1*(1.+(COND1/2.)*
     1      (1.+(COND1/3.)*(1.+(COND1/4.))))
  502       IF (OPTION.EQ.0.OR.OPTION.EQ.2) GO TO 505
C
C           NOW CALCULATE THE FRESNEL REFLECTANCE AT THIS SCAN ANGLE
C           NEEDED TO FIND THE REFLECTED SKY RADIANCE.
C
```

TABLE 2 (Cont.)

```
      IF (THETA) 58, 59, 58
   58 THETTA=ABS(THETA)
      REFRAC=ARSIN(SIN(THETTA)*1./INDEX)
      AX=THETTA-REFRAC
      BX=THETTA+REFRAC
      SINA=SIN(AX)
      SINB=SIN(BX)
      TANA=TAN(AX)
      TANB=TAN(BX)
      FRES(IP)=0.5*((SINA*SINA)/(SINB*SINB)+(TANA*TANA)/(TANB*TANB))
      GO TO 310
   59 FRES(IP)=FRESO
  310 CONTINUE
C
C     CALCULATE THE OTHER SCAN ANGLE DEPENDENT QUANTITIES NEEDED
C     TO FIND THE REFLECTED SKY RADIANCE.
C
      ARGSKY=FMU-FPHI*ROOT
      PFSKY=PF(ARGSKY,I,TR(I),TAS(I))
      EXPO2=TAU(I)/MU
      MUFAC2=(MUO-MU)/MUO
      COND2=EXPO2*MUFAC2
      IF (ABS(COND2).LT.COND) GO TO 503
C
C     CALCULATE THE REFLECTED SKY RADIANCE
C
      LRSKY(I,IP)=FRES(IP)*(CONST/MUFAC2)*PFSKY*EFACT(I,IP)*
     1                     (EFACTS-EXP(-EXPO2))
      GO TO 505
C
C     EITHER MU AND MUO OR TAU(I) AND TAUZ(I) ARE TOO CLOSE TOGETHER
C     SO THE FOURTH ORDER EXPANSION OF THE REFLECTED SKY RADIANCE
C     MUST BE USED.
C
  503 LRSKY(I,IP)=FRES(IP)*CONST*PFSKY*EFACT(I,IP)*EFACTS*EXPO2*(1.
     1                  -(COND2/2.)*(1.-(COND2/3.)*(1.-(COND2/4.))
     2                  ))
  505 IF (OPTION.LT.2) GO TO 2019
C
C     CALCULATE THE SCAN ANGLE DEPENDENT QUANTITIES NEEDED TO FIND
C     THE PATH RADIANCE GENERATED BY THE VIRTUAL SUN.
C
      ARGVIR=FMU-FPHI*ROOT
      PFVIR=PF(ARGVIR,I,TR(I),TAS(I))
      MUFAC2=(MUO-MU)/MUO
      COND3=EXPO1*MUFAC2
      IF (ABS(COND3).LT.COND) GO TO 506
C
C     CALCULATE THE PATH RADIANCE GENERATED BY THE VIRTUAL SUN.
C
      LVIRP(I,IP)=FRESUN*(CONST/MUFAC2)*PFVIR*EFACTS*(1./EFACTO -
     1                 EFACT(I,IP))
      GO TO 2019
C
C     EITHER MU AND MUO OR TAU(I) AND TAUZ(I) ARE TOO CLOSE TOGETHER
C     SO WE USE THE EXPANSION OF THE VIRTUAL PATH RADIANCE.
C
  506 LVIRP(I,IP)=FRESUN*CONST*PFVIR*EFACTS*EFACT(I,IP)*EXPO1*(1.+
     1            (COND3/2.)*(1.+(COND3/3.)*(1.+(COND3/4.))))
      GO TO 2019
```

TABLE 2 (Cont.)

```
      510     CONTINUE
C
C             CALCULATE THE SCAN ANGLE DEPENDENT QUANTITIES NEEDED TO FIND
C             THE MULTIPLY SCATTERED RADIANCE.
C
              IF (OM(I) .GT. OML) GO TO 52
C               DEFINE SINGULARITIES
                SING1 = NUSQ(I) - MUSQ
                SING2 = NUSQ(I) - CO2*CO2*MUSQ
                IF (ABS(SING1).GT.EPS .AND. ABS(SING2).GT.EPS) GO TO 55
                  WRITE (QUERR,380)
  380             FORMAT('-ATMSFR: *****ERROR-- SINGULARITY EXISTS IN EQUATI
     1            ONS*****')
                  ATHET = 57.29578*THETA
                  WRITE (QUERR,385) ATHET
  385             FORMAT(' ATMSFR:         SINGULAR AT THETA=',F7.4)
                  GO TO 2019
   55           CONTINUE
                PF1 = PF(ARG,I,TR(I), TAS(I))
                PF2 = PF(-ARG,I,TR(I), TAS(I))
                EFACT(I,IP) = EXP(-SIG(I)/MU)
                MFACT = MU * EFACT(I,IP)
C               CALCULATE PATH RADIANCE
                LPATH(I,IP) = LAMPP(I) *
     1           (A(I)*(AT(I)-BT(I)*MU + MFACT) *PF1
     2          +(ATP(I) -BTP(I)*MU -MUO*EFACT(I,IP) +B(I)*MFACT)*PF2)/SING1
     3          +PHIP(I)*
     4          (ATPP(I) +BTPP(I)*MU -CTPP(I)*EFACT(I,IP) -DTPP(I)*MFACT)
     5          /SING2
                GO TO 2019
  52          CONTINUE
C               CALCULATE PHASE FUNCTIONS
                PF1 = PF(ARG,I,TR(I), TAS(I))
                PF2 = PF(-ARG,I,TR(I), TAS(I))
                EFACT(I,IP) = EXP(-SIG(I)/MU)
                CFACT = 1.0 -EFACT(I,IP)
C               CALCULATE PATH RADIANCE
                LPATH(I,IP) = FP(I) *
     1          ((SIG(I) -MU*CFACT)*PF1 + (SIG(I) + (D(I)-MU)*CFACT)*PF
     2          2 + (ALPHA(I) + G(I)*MU)*CFACT)
 2019       CONTINUE
  10      CONTINUE
C
C             ECHO MORE QUANTITIES FOR THE USER'S CONVENIENCE.
C
          WRITE(QUPRNT,555)(ETA(I),I=1,QNCHAN)
  555 FORMAT('- ANISOTROPY PARAMETER',10F10.5)
          WRITE(QUPRNT,291)
  291 FORMAT('                (ETA)')
          WRITE(QUPRNT,282)(TAUZ(I),I=1,QNCHAN)
  282 FORMAT('- OPTICAL DEPTH          ',10F10.5)
          WRITE(QUPRNT,297)(E(I),I=1,QNCHAN)
  297 FORMAT('- TOTAL IRRADIANCE',4X,10F10.5)
          WRITE(QUPRNT,298)
  298 FORMAT('           ON SURFACE')
          WRITE( QUPRNT,370)(ED(I),I=1,QNCHAN)
  370 FORMAT('- DIRECT IRRADIANCE     ',10F10.5)
          WRITE(QUPRNT,371)
  371 FORMAT('           ON SURFACE')
          RETURN
```

TABLE 2 (Cont.)

```
C**********************************************************************
C  QSTEP=8 -- NEXT LINE TO BE PROCESSED:
C**********************************************************************
 8     CONTINUE
C      IF WE ARE PRINTING RADIOMETRIC QUANTITIES, START EACH LINE ON
C        A NEW PAGE
       IF(LSW.EQ.6) WRITE(QUPRNT,400)
 400   FORMAT('1')
C      LOOP FOR EACH PIXEL--QNSS=NUMBER OF PIXELS
       DO 1009 IP=FSTP,LSTP,PTINC
C        TEST "BAD DATA" FLAG FOR THIS PIXEL.  IF NON-ZERO, DON'T PROCESS.
         IF (CONTRL(IP) .NE. 0) GO TO 2009
           DO 3009 IW=1,QNCHAN
C            TOTAL RADIANCE (EXPERIMENTAL) = L(IW,IP)
             LBEAM(IW) = L(IW,IP) - LPATH(IW,IP)
             IF (SCATT.EQ.0) GO TO 520
             IF (OPTION.EQ.1.OR.OPTION.EQ.3)LBEAM(IW)=LBEAM(IW)-LRSKY(IW,
     1                                                                IP)
             IF (OPTION.GE.2)LBEAM(IW)=LBEAM(IW)-LVIRP(IW,IP)
  520        CONTINUE
             IF (L(IW,IP).EQ.0) LBEAM(IW) = 0
C            CALCULATE SURFACE RADIANCE
             LSURF(IW) =  LBEAM(IW)/EFACT(IW,IP)
C            CALCULATE INTRINSIC RADIANCE
             LINTR(IW) = FE(IW)*LSURF(IW)
C            CALCULATE SURFACE REFLECTANCE
             RHOS(IW) = LSURF(IW)/E(IW)
             GO TO (71,72,73,74,75,76),LSW
 71          L(IW,IP) = LPATH(IW,IP)
             GO TO 60
 72          L(IW,IP) = LBEAM(IW)
             GO TO 60
 73          L(IW,IP) = LSURF(IW)
             GO TO 60
 74          L(IW,IP) = LINTR(IW)
             GO TO 60
 75          L(IW,IP) = RHOS(IW)
             GO TO 60
 76          CONTINUE
             THETA = (QBANG-QDANG*(IP-1)) *180/PI
 60        CONTINUE
 3009      CONTINUE
           IF (LSW.NE.6) GO TO 3019
C            PRINT RADIOMETRIC QUANTITIES
             IF(SCATT.EQ.0.OR.OPTION.EQ.0.OR.OPTION.EQ.2)WRITE(QUPRNT,410
     1                                                )QLINE,IP,THETA
  410        FORMAT(5X,'LINE NUMBER',I6,5X,'PIXEL NUMBER',I4,5X,
     1              'SCAN ANGLE=',F7.3,'DEGREES')
             IF(SCATT.NE.0.AND.(OPTION.EQ.  OR.OPTION.EQ.3))WRITE(QUPRNT,
     1                                           411)QLINE,IP,THETA,FRES(IP)
  411        FORMAT(5X,'LINE NUMBER',I6,5X,'PIXEL NUMBER',I4,5X,
     1              'SCAN ANGLE=',F7.3,'DEGREES      FRESNEL REFLECTANCE='
     2              ,2F6.3)
             WRITE (QUPRNT,420)
 420         FORMAT('O',14X,'1',9X,'2',9X,'3',9X,'4',9X,'5',9X,'6',
     1       9X,'7',9X,'8',9X,'9',9X,'10')
             WRITE (QUPRNT,425) (L(IW,IP),IW=1,QNCHAN)
  425        FORMAT('O LTOT   ',10F10.5)
             WRITE (QUPRNT,430) (LPATH(IW,IP),IW=1,QNCHAN)
  430        FORMAT('  LPATH  ',10F10.5)
```

ORIGINAL PAGE IS
OF POOR QUALITY

TABLE 2 (Cont.)

```
                IF (SCATT.EQ.0)GO TO 433
                IF(OPTION.EQ.1.OR.OPTION.EQ.3)WRITE(QUPRNT,431)(LRSKY(IW,IP)
     1                                                 ,IW=1,QNCHAN)
  431           FORMAT('  LRSKY ',10F10.5)
                IF(OPTION.GE.2)WRITE(QUPRNT,432)(LVIRP(IW,IP),IW=1,QNCHAN)
  432           FORMAT('  LVIRP ',10F10.5)
  433           WRITE(QUPRNT,434)(EFACT(IW,IP),IW=1,QNCHAN)
  434           FORMAT('   TRANS ',10F10.5)
                WRITE (QUPRNT,435) LBEAM
  435           FORMAT('  LBEAM ',10F10.5)
                WRITE (QUPRNT,440) LSURF
  440           FORMAT('  LSURF ',10F10.5)
                WRITE (QUPRNT,445) LINTR
  445           FORMAT('  LINTR ',10F10.5)
                WRITE (QUPRNT,450) RHOS
  450           FORMAT('  RHOS  ',10F10.5/'0')
C               SET QBNONE TRUE TO TELL ANY FOLLOWING MODULES THAT NO OUTPUT
C                DATA ARE PRESENT.
                QBNONE = .TRUE.
 3019         CONTINUE
 2009       CONTINUE
 1009   CONTINUE
        RETURN
        END
END OF FILE
```

The user must also define the center wavelengths (μm) of the multispectral scanner and the corresponding values of the surface background albedo (values from zero to one). Also, the center wavelengths (μm) of the surface radiometers and the corresponding optical thicknesses must be known. It should be noted that the optical thicknesses used should be those measured as closely as possible in time with the multispectral data.

5.4 MODEL CALCULATIONS

In this section we present several examples of the radiances for the various components. Because our main interest is in the radiance components as a function of scan angle and visibility, we will present the results of the calculations in terms of these parameters.

Figure 10 depicts the variation in the singly-scattered reflected sky radiance at the sensor as a function of the nadir scan angle and visibility. In this example the solar zenith angle is 45° and the scan plane is perpendicular to the solar plane. The curves which result are a combination of the variation of the sky radiance, the transmittance from the surface to the sensor, and the Fresnel reflectance of the water surface. For a practical scanner with a maximum scan angle of about 45° the curves indicate that one would not observe the large radiance peaks at the large angles.

In Figure 11 we display the corresponding path radiance as a result of singly-scattered radiation from the reflection of the sun in the water. In this case the radiance peaks do not exist at the large scan angles.

In Figure 12 we illustrate the relative magnitudes of the various radiation components as a function of scan angle for a moderately hazy atmosphere. The virtual sun path radiance is the smallest value and the multiply scattered sky radiance is the largest value.

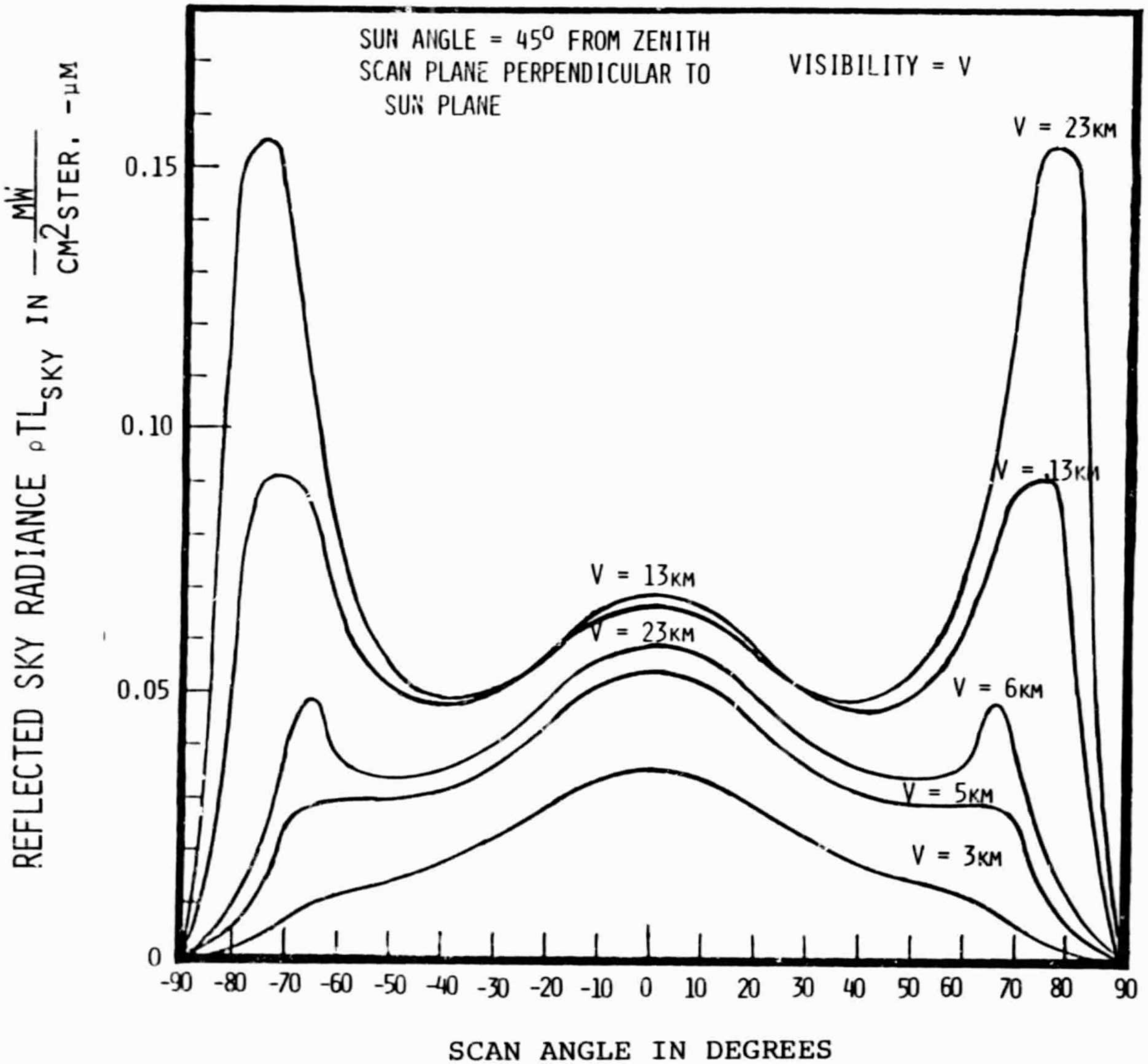

Figure 10. Singly-Scattered Reflected Sky Radiance at Sensor for a Wavelength of 0.55μM

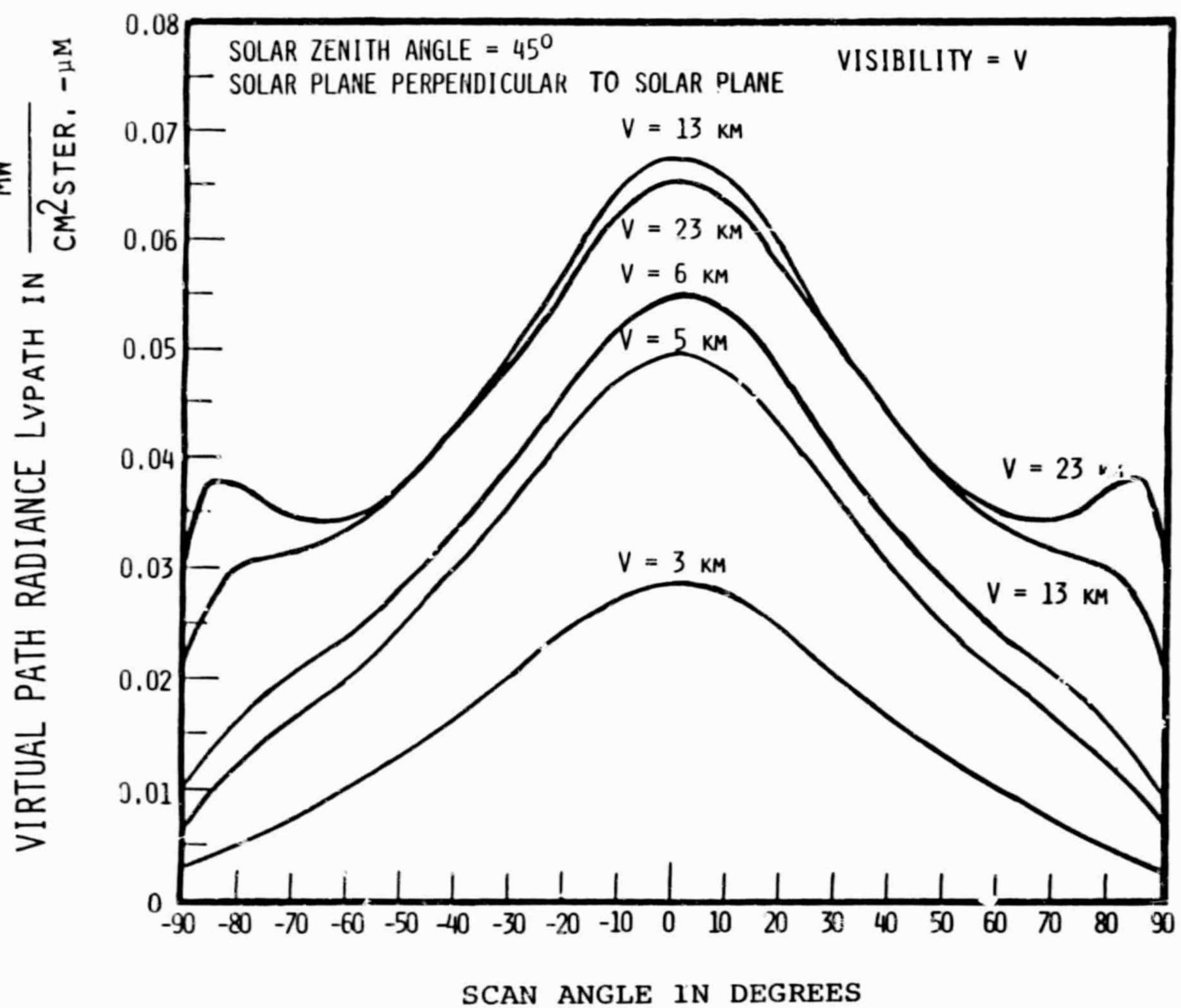

Figure 11. Singly-Scattered Virtual Path Radiance at Sensor for a Wavelength of 0.55μM

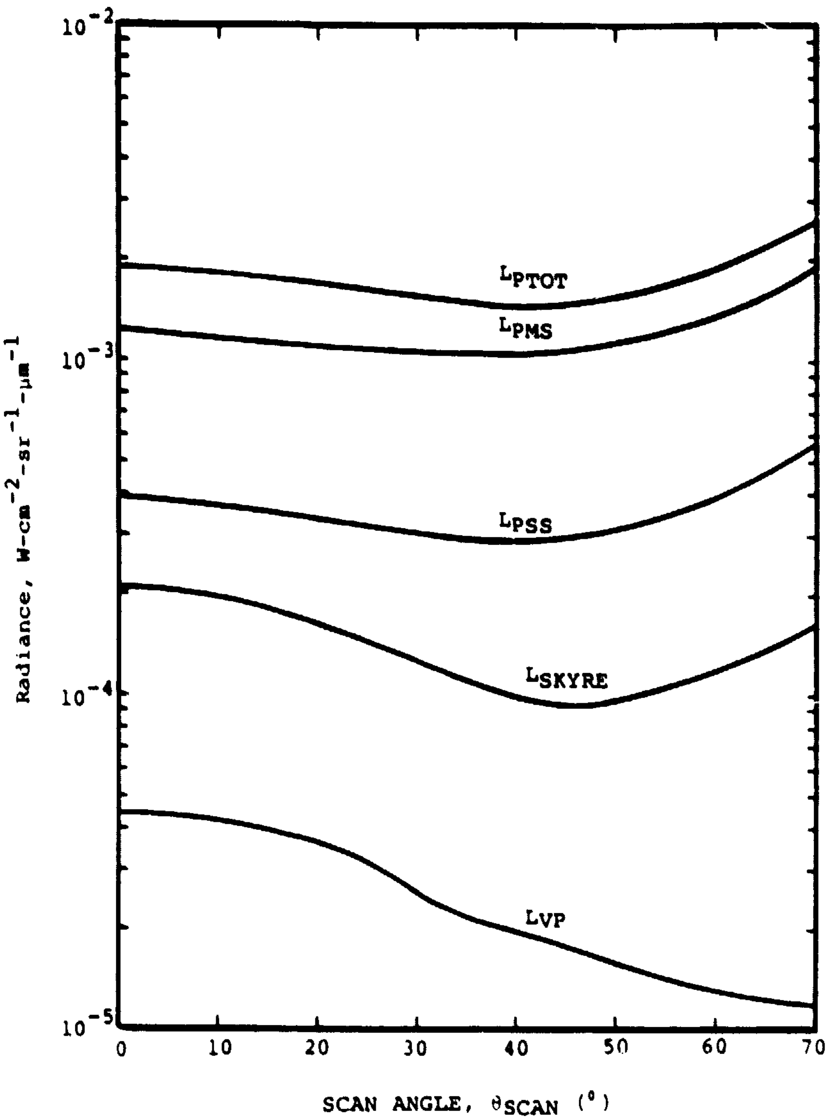

L_{VP} = virtual sun path radiance;
L_{SKYRE} = reflected sky radiance;
L_{PSS} = singly scattered path radiance;
L_{PMS} = multiply scattered path radiance;
L_{PTOT} = L_{VP} + L_{SKYRE} + L_{PSS} + L_{PMS}.

Figure 12. SURFACE AND PATH RADIANCE COMPONENTS DETECTED BY SENSOR AT OPTICAL DEPTH OF τ = 0.346 AS A FUNCTION OF SCAN ANGLE, θ_{SCAN}. SCAN PLANE $\perp$ SOLAR PLANE, θ_{SUN} = 30°, λ = 0.55 µM, PHASE FUNCTION = CONTINENTAL REFRACTIVE INDEX 1.5 - 0.01i, VISIBILITY = 10 KM.

In Figure 13 we indicate the variation in the ratio of the singly-scattered sky radiance to the singly-scattered path radiance as a function of the optical depth τ of the sensor. As the curves illustrate, the reflected sky radiance component is relatively more important for the larger optical depths.

Figure 14 illustrates the variation in the ratio of the virtual sun path radiance to the singly-scattered path radiance with scan angle for four optical depths.

Figure 15 depicts the large ratio of the multiply-scattered component to the singly-scattered path radiance component as a function of optical depth and scan angle.

Because optical thickness or visibility is of major importance in remote sensing investigations, we want to consider the variation of the radiance components with respect to visibility. This effect is illustrated in Figure 16 for three different atmospheres. We chose the continental aerosol because it more nearly represents the type which would be found over the Great Lakes. The three refractive indices are: 1.5-0.0i which corresponds to a "clean" haze, i.e., one where there is no absorption; 1.5-0.01i which corresponds to a haze with some aerosol absorption; and 1.5-0.1i, a complex index of refraction which corresponds to a haze with more absorption. As the curves indicate, an absorbing haze or one which corresponds to considerable air pollution gives rise to a large ratio of reflected sky radiance relative to the singly-scattered path radiance.

The effect of the complex index of refraction is also evident in the ratio of the virtual sun path radiance to the singly-scattered path radiance as indicated in Figure 17.

Finally, we illustrate in Figure 18 the variation of various combinations of ratios in terms of the visibility for a refractive index of 1.5-0.01i.

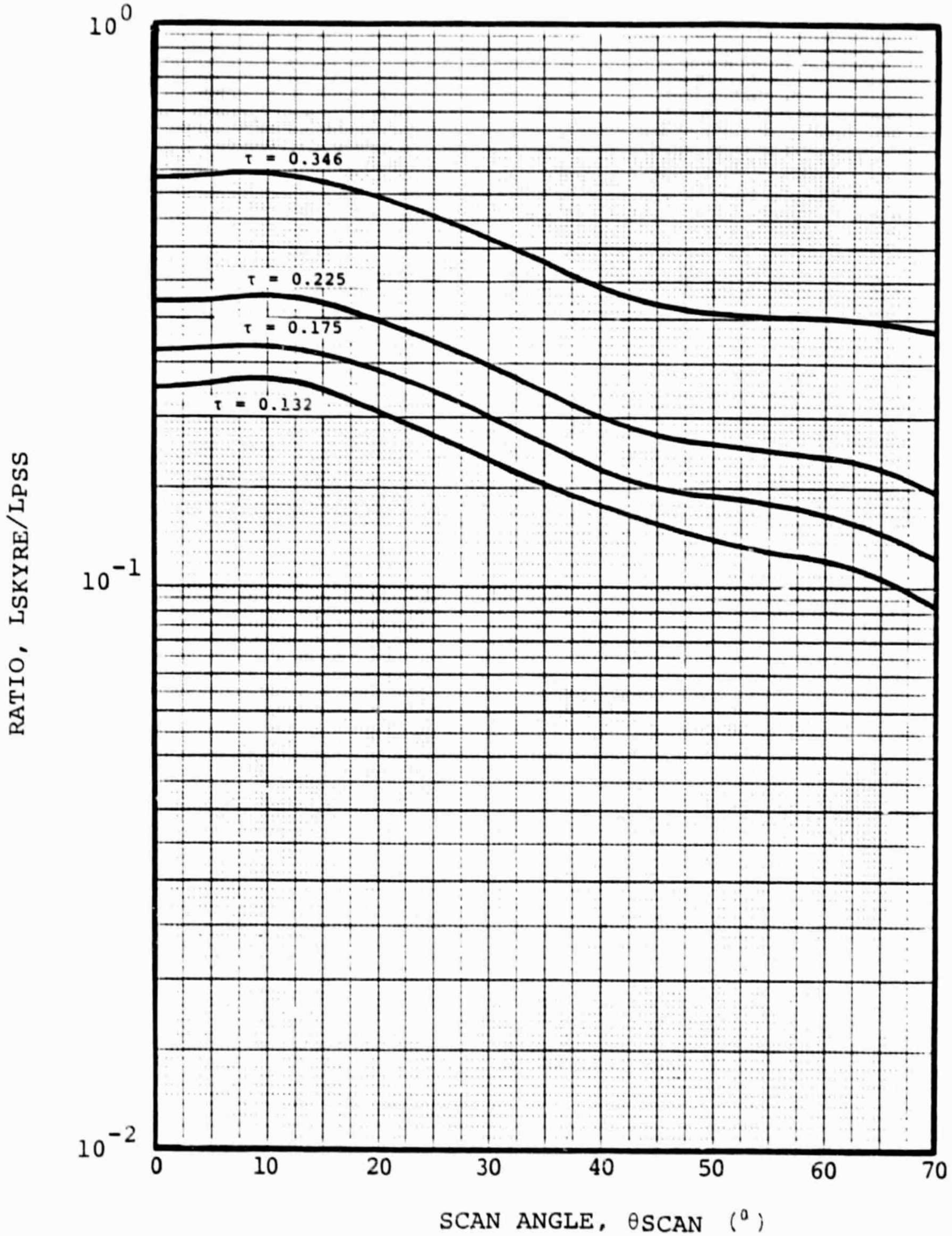

FIGURE 13. RATIO OF REFLECTED SINGLY SCATTERED SKY RADIANCE TO SINGLY SCATTERED PATH RADIANCE AS A FUNCTION OF SCAN ANGLE, θ_{SCAN}, FOR OPTICAL DEPTH, τ, OF THE SENSOR OF 0.132, 0.175, 0.225 and 0.346. SCAN PLANE $\perp$ SOLAR PLANE, PHASE FUNCTION = CONTINENTAL REFRACTIVE INDEX 1.5 - 0.01i, VISIBILITY = 10 KM, λ = 0.55 μM, $\theta_{SUN} = 30^0$.

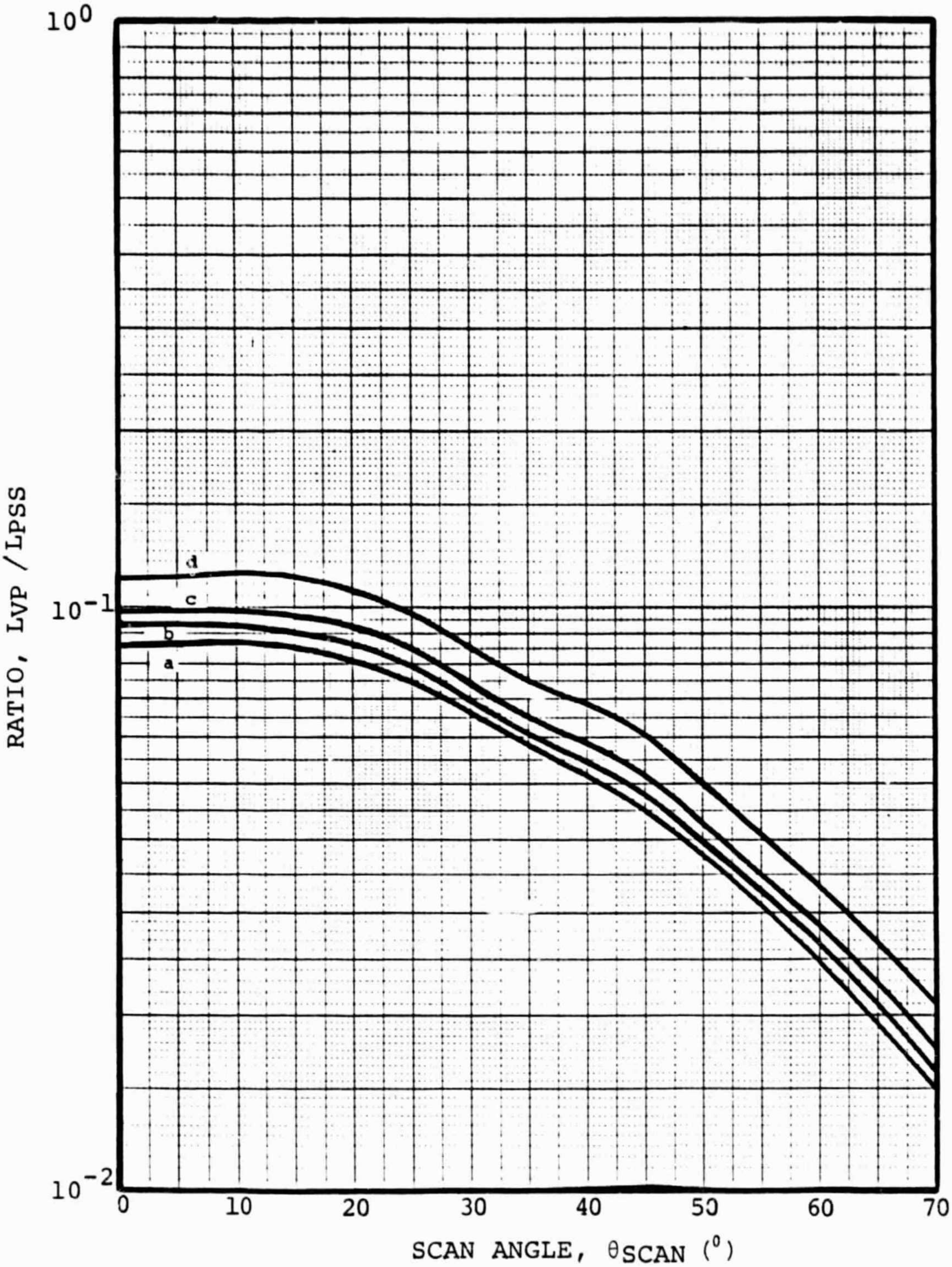

FIGURE 14. RATIO OF SINGLY SCATTERED PATH RADIANCE FROM THE VIRTUAL SUN, L_{VP}, TO SINGLY SCATTERED PATH RADIANCE, L_{PSS}, AS A FUNCTION OF SCAN ANGLE, θ_{SCAN}, FOR OPTICAL DEPTHS, τ, OF THE SENSOR OF A) 0.132, B) 0.175, C) 0.225 AND D) 0.346. SCAN PLANE $\perp$ SOLAR PLANE, PHASE FUNCTION = CONTINENTAL REFRACTIVE INDEX 1.5 - 0.01i, VISIBILITY = 10 KM, λ = 0.55 μM, $\theta_{SUN} = 30^0$.

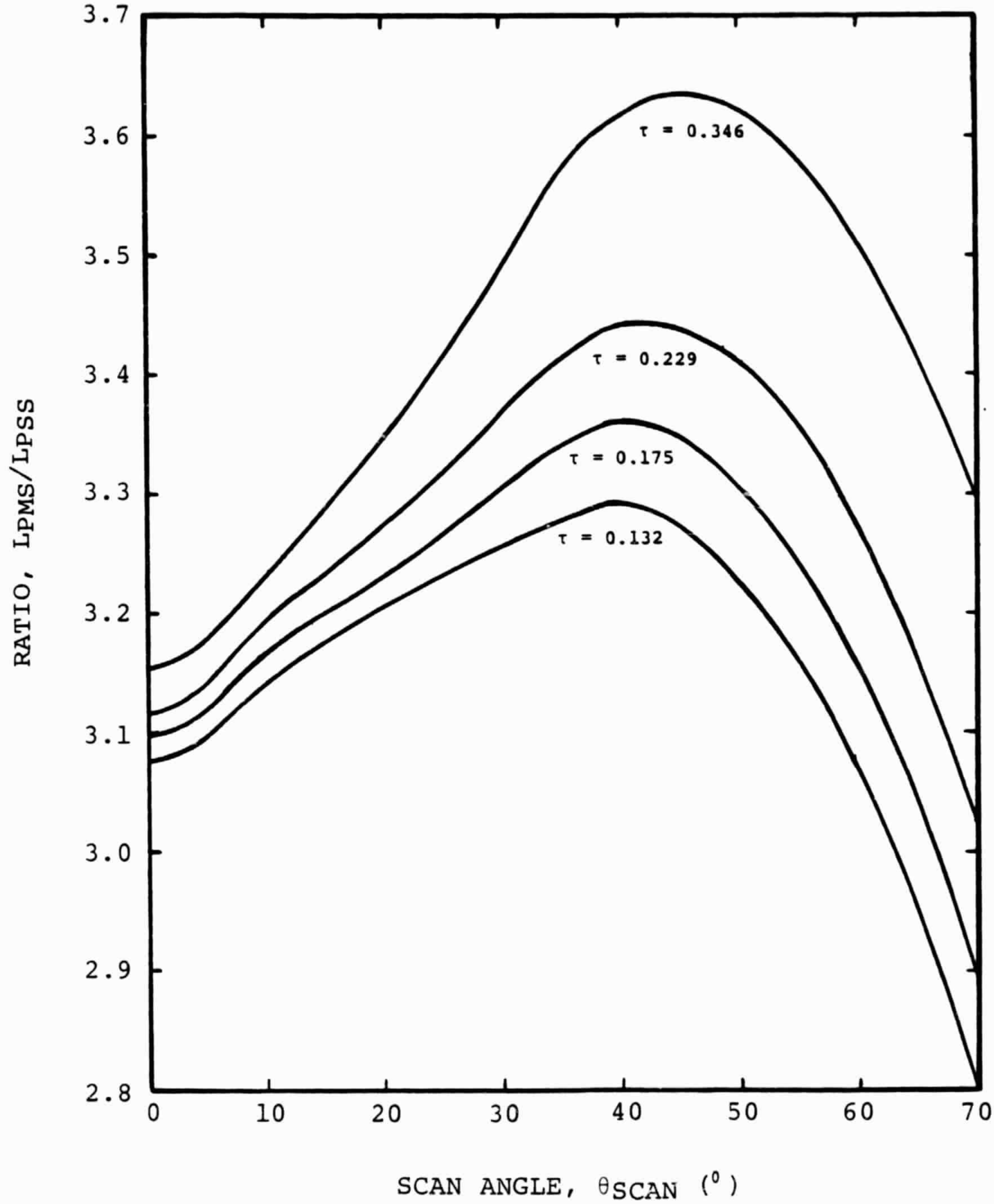

FIGURE 15. RATIO OF MULTIPLY SCATTERED PATH RADIANCE, L_{PMS}, TO SINGLY SCATTERED PATH RADIANCE, L_{PSS}, AS A FUNCTION OF SCAN ANGLE, θ_{SCAN}, FOR OPTICAL DEPTHS, τ, OF THE SENSOR OF 0.132, 0.175, 0.229, 0.346. SCAN PLANE $\perp$ SOLAR PLANE, VISIBILITY = 10 KM, PHASE FUNCTION = CONTINENTAL REFRACTIVE INDEX 1.5 - 0.01i, λ = 0.55 μM, θ_{SUN} = 30°.

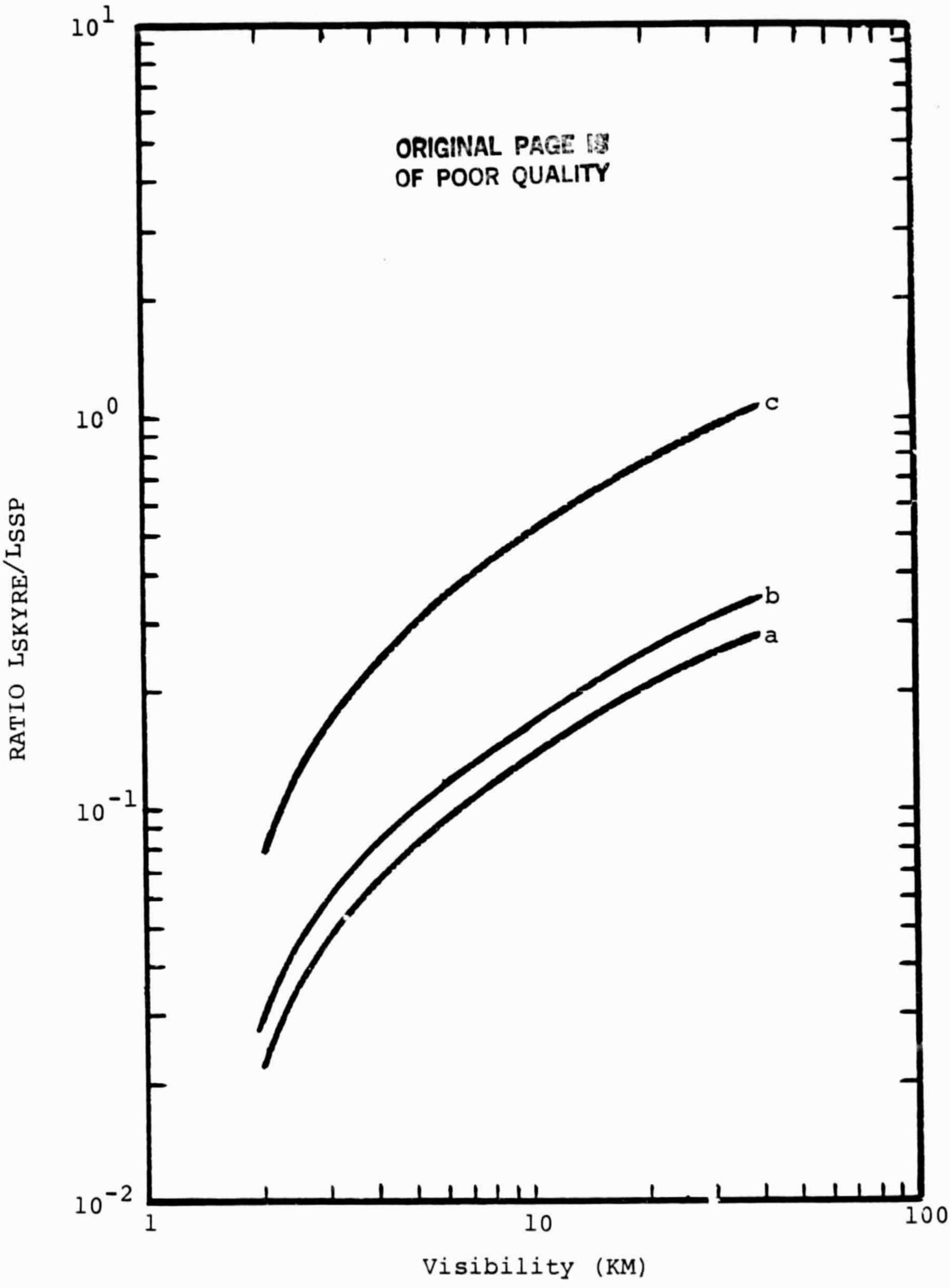

Figure 16. RATIO OF REFLECTED SKY RADIANCE TO SINGLY SCATTERED PATH RADIANCE FOR THREE CONTINENTAL AEROSOL MODELS: a) 1.5 - 0.0i, b) 1.5 - 0.01i, and c) 1.5 - 0.1i AS A FUNCTION OF ATMOSPHERIC VISIBILITY. SCAN PLANE ⊥ SOLAR PLANE, $\theta_{SUN} = 30^0$, $\lambda = 0.55$ μM.

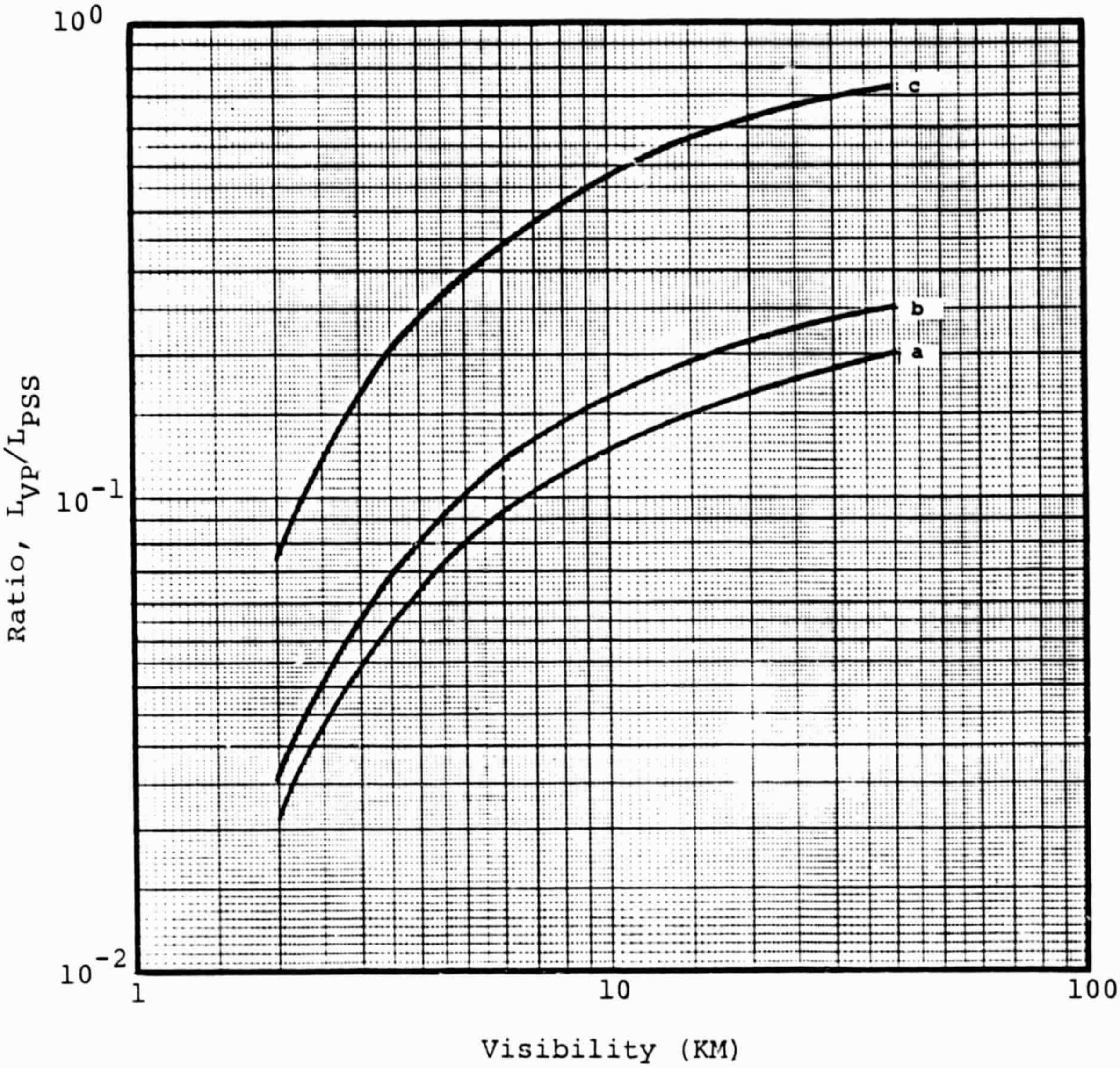

FIGURE 17. RATIO OF SINGLY SCATTERED PATH RADIANCE FROM THE VIRTUAL SUN, L_{VP}, TO SINGLY SCATTERED PATH RADIANCE, L_{PSS}, AS A FUNCTION OF ATMOSPHERIC VISIBILITY FOR THREE CONTINENTAL AEROSOL MODELS WITH REFRACTIVE INDICES OF a) 1.5 - 0.0i, b) 1.5 - 0.01i, and c) 1.5 - 0.1i. λ = 0.55 μM, θ_{SUN} = 30°, θ_{SCAN} = 0°.

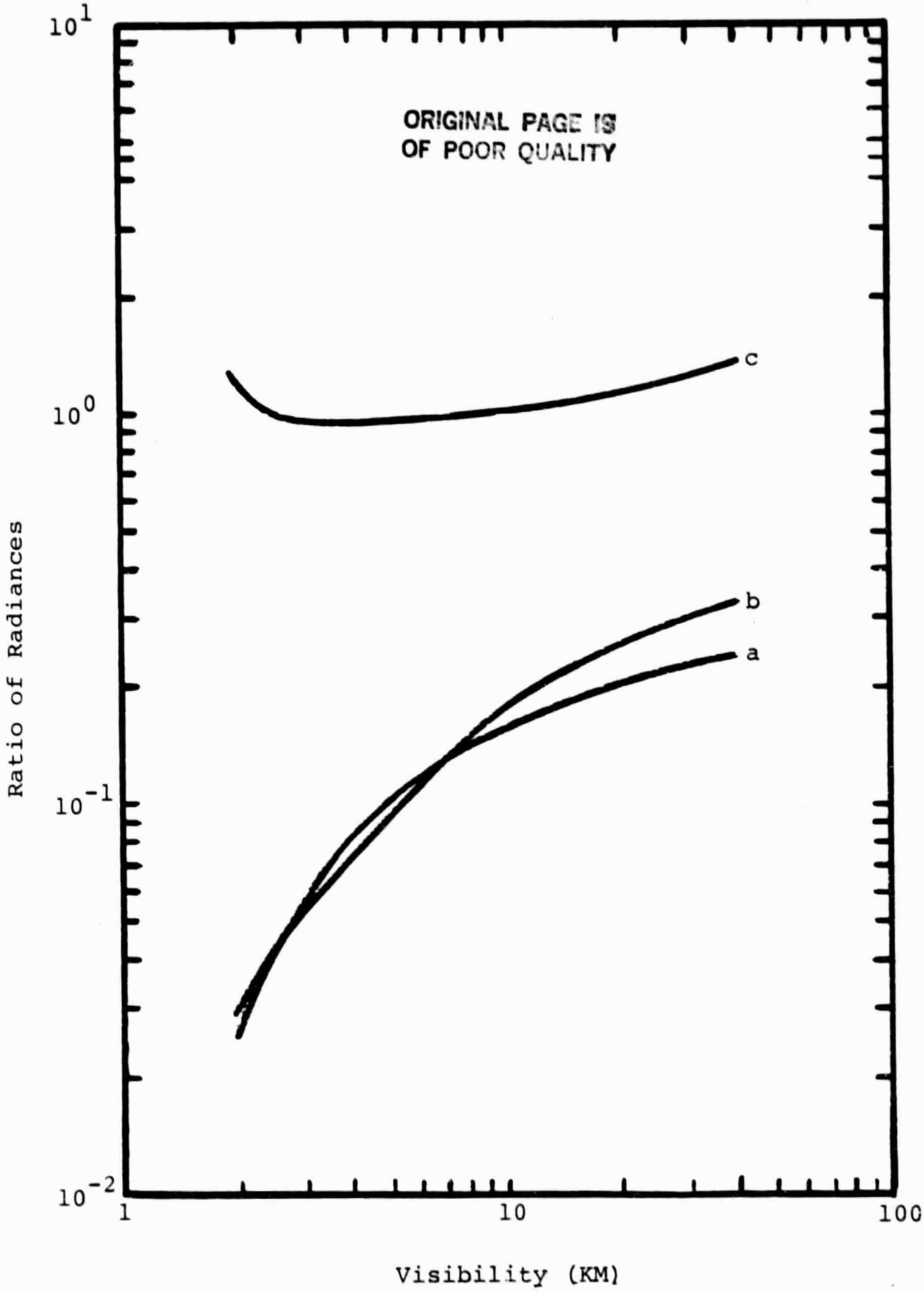

L_{VP} = virtual sun path radiance;

L_{PSS} = singly scattered path radiance;

L_{SKYRE} = reflected sky radiance.

FIGURE 18. RATIOS OF (a) L_{VP}/L_{PSS}, (b) L_{SKYRE}/L_{PSS}, (c) L_{SKYRE}/L_{VP} AS A FUNCTION OF VISIBILITY (KM). λ = 0.55 µM, $\theta_{SUN} = 30^0$, $\theta_{SCAN} = 0^0$, AEROSOL MODEL = CONTINENTAL REFRACTIVE INDEX 1.5 - 0.01i.

6
CONCLUSIONS AND RECOMMENDATIONS

The problem of developing an atmospheric correction algorithm for remote sensing is an old and difficult one. The main difficulty lies in not being able to have available sufficient data which can be used to specify the values of the relevant atmospheric parameters The problem is all the more difficult in the case of the remote sensing of water bodies because of the low signal-to-noise ratio involved. In this investigation we have extended an existing computer algorithm so as to include additional radiation components. The original algorithm included the path radiance which arises from the singly-scattered solar radiation in the atmosphere. We have now included the radiance which arises from the sky radiation which is reflected by the water surface and is then attenuated as it propagates from the surface to the sensor. In addition, we have included the path radiance component which arises from the single scattering of radiation as a result of a virtual sun, i.e., of the sun's reflection in the water. It should be realized that this component is always present regardless of the scan plane, i.e., it does not only occur when the scanner is looking at the specular angle. In addition to these components, we have also included a multiple-scattering approximation. It should be realized, however, that the multiple scattering applies only to an atmosphere with the sun as a source. Another multiple scattering calculation should be performed to include the effect due to the virtual sun.

The general result of all these calculations indicates that the various components are all about equal in magnitude but that there is considerable variation with respect to scan angle and visibility. Also, it appears that the multiply-scattered component is of major significance.

It must be pointed out that the objective of this investigation is to provide an algorithm for the correction of remotely sensed data for atmospheric effects so that one can extract from the multispectral data the radiance which is characteristic of the water itself. In our investigation we have dealt with the water surface as a flat, specular reflector, which in general is not true. A wind-roughened surface will be characterized by a complex wave structure which leads to a more complicated representation of the reflected and virtual sun radiances than presented in this report. A further investigation should be conducted to model the water surface in terms of wind speed and a stochastic representation of the reflecting facets of the water surface. If this is done, then a more realistic model could be developed which should provide better values for the sky-reflected and the virtual sun path radiances. It may even be possible to establish a method for the determination of wind speed by observing the average radiance as a function of the instantaneous field of view.

A further recommendation is to improve the accuracy of the algorithm by including a more detailed calculation of the multiply-scattered path radiance, both for the direct sun as a source and for the virtual sun as a source.

REFERENCES

1. Austin, R. W., 1974: The Remote Sensing of Spectral Radiance from Below the Ocean Surface. In Optical Aspects of Oceanography, N. G. Jerlov & E. S. Nielsen (eds.) Academic Press, New York, pp 317-344.

2. Jerlov, N. G., 1976: Marine Optics. Elsevier, New York, p. 229.

3. Plass, G. N. and Kattawar, G. W., 1969: Radiative Transfer in the Atmosphere-Ocean System. Applied Optics, 8, pp 455-466.

4. Kullenberg, G., 1974: Observed and Computed Scattering Functions. In Optical Aspects of Oceanography, Academic Press, N. G. Jerlov and E. S. Nielsen (eds.), New York, pp 25-49.

5. Beardsley, G. F., Jr., 1968: Mueller Scattering Matrix of Sea Water, J. Opt. Soc. Am, 58, pp. 52-57.

6. Holland, A. C. and Gagne, G., 1970: The Scattering of Polarized Light by Polydisperse Systems of Irregular Particles, Applied Optics, 9, pp 1113-1121.

7. Cox. C. and Munk, W., 1956: Slopes of the Sea Surface Deduced from Photographs of Sun Glitter, Bull Scripps Inst. Oceangr. University of California, 6, pp 401-488.

8. Kondratyer, K. Y., 1969: Radiation in the Atmosphere, International Geophysics Series, Academic Press, New York 912 pages.

9. Burt, W. V., 1954a: Albedo Over Wind-Roughened Water, J. Meteorol. II, pp. 283-290.

10. Plass, G. N., Kattawar, G. W. and Guinn, J. A., Jr., 1975: Radiative Transfer in the Earth's Atmosphere and Ocean: Influence of Waves, Applied Optics, 14, pp. 1924-1936.

11. Cox. C. S., 1974: Refraction and Reflection at the Light Surface. In Optical Aspects of Oceanography, Academic Press, N. G. Jerlov and E. S. Nielsen (eds.), New York, pp. 51-76.

12. Duntley, S. Q., 1950: The Visibility of Submerged Objects: Part I. Optical Effects of Water Waves. Ref. Visibility Lab., Mass. Institute of Technology, Dec. 15, 1950; U.S. Off. Naval Research Rep. No. N5 ori-07831.

13. Cox. C. S., and Munk, W., 1954: Statistics of the Sea Surface Derived from Sun Glitter, Journal of Marine Research, 13, pp. 198-227.

REFERENCES (Continued)

14. Turner, R. E., 1974: Radiative Transfer in Real Atmospheres, NASA CR-ERIM 190100-24-T, Final Report.

15. Turner, R. E., 1976: Investigation of Earth's Albedo Using Skylab Data, NASA CR-ERIM 102200-20-F, Final Report.

16. Turner, R. E., 1977: Atmospheric Transformation of Multispectral Remote Sensor Data, NASA CR-135338.

17. U.S. Standard Atmosphere, 1976: NOAA-S/T 76-1562, U.S. Government Printing Office.